Supporting Information

Scalable Production of Graphene Oxide Using a 3D-Printed Packed-Bed Electrochemical Reactor with a Boron-Doped Diamond Electrode

Sean E. Lowe,[†] Ge Shi,[†] Yubai Zhang,[†] Jiadong Qin,[†] Shujun Wang,[†] Alexander Uijtendaal,[†] Jiqing Sun,[†] Lixue Jiang,[†] Shuaiyu Jiang,[†] Dongchen Qi,[§] Mohammad Al-Mamun,[†] Porun Liu,[†] Yu Lin Zhong,[*†] Huijun Zhao[*†]

[†] Centre for Clean Environment and Energy, School of Environment and Science, Gold Coast Campus, Griffith University, Gold Coast, QLD 4222, Australia

[§] School of Chemistry, Physics and Mechanical Engineering, Queensland University of Technology, Brisbane, Queensland 4001, Australia

Department of Chemistry and Physics, La Trobe University, Melbourne, Victoria 3086, Australia

*E-mail: y.zhong@griffith.edu.au, *E-mail: h.zhao@griffith.edu.au

Expanded experimental section

The experimental methods of the main text are annotated here with additional details.

Fabrication of Electrochemical Reactors

3D-printed components for the reactors were designed in Autodesk 123D Design. For the smaller glass reactor, a conical weight platform and the flanges used to clamp the reactor to the boron-doped diamond (or other working electrode) plate were printed using a semitransparent 1.75-mm-diameter ABS filament (Verbatim Americas LLC, Charlotte, NC). The cylindrical graphite press was printed with a semitransparent 1.75-mm-diameter PVDF filament (Apium Additive Technologies, Karlsruhe, Germany). All parts for the larger polypropylene (PP) reactor were printed using a 1.75-mm-diameter semitransparent PP filament (Verbatim Americas LLC, Charlotte, NC, US). All parts were printed using a Makergear M2 or M3 3D printer (Beachwood, OH).

The smaller reactor was assembled by first gluing a glass tube (cut from a standard 14 mm internal diameter test tube) to the 3D printed clamping flanges with epoxy resin. The tube was then clamped onto a metal or coated metal working electrode substrate (in this case, a platinum (Pt) foil, mixed metal oxide (MMO) plate, or boron-doped diamond (BDD) plate). Glass was used in the smaller reactor and for fundamental studies to allow us to visually monitor the reaction. Three layers of Parafilm (Parafilm M, Bemis, Neenah, WI) with a 13-mm-diameter hole punched in them were placed between the glass tube and the underlying metal to form a seal. The BDD plate had dimensions 100 mm (length) × 20 mm (width) × 2 mm (height) and was composed of niobium coated with CVD-grown polycrystalline BDD (Diaccon GmBH, Fürth, Germany). The thickness of the BDD film was 12-18 μm. The Pt anode was a foil of 0.05 mm thickness (Item 690-996-10, Goodfellow, Cambridge, UK). The iridium-tantalum MMO was a 100 × 100 mm titanium plate coated with the active anode material (Baoji Qixin Titanium Company, Ltd, Baoji City, China).

In this design, flake graphite was poured into the glass tube to form a packed bed. Three glass microfiber filters (pore size 0.7 μm, Whatman brand from GE Healthcare, Chicago, IL; Catalog No. 1825-047) were cut to fit the shape of the glass tube and stacked on top of the graphite. A 3D printed, weighted press was then placed on top of the glass fiber membranes to hold the graphite down. The graphite press had rectangular gratings of approximately 2.5 mm thickness at the bottom to allow electrolyte and gas flow between the graphite bed and the bulk solution. The counter electrode consisted of a 33 cm loop of 0.25 mm diameter Pt wire (Item 850-988-64, Goodfellow, Cambridge, U.K.). The Pt wire loop was fed into the graphite press until it was suspended approximately 4 mm from the glass fiber membrane. The working and counter electrodes were connected to a Gamry Interface 1000 potentiostat (Gamry Instruments, Warminster, PA).

The larger rectangular PP reactor (schematic in Figure S11) used the same BDD working electrode, but the graphite covered a larger area of the plate. The counter electrode was a 186 cm Pt wire loop made of the same material used previously and was again suspended roughly 4 mm above the bottom of the graphite press. The graphite press was 3D printed in PP and had square holes of approximately 2 mm width at the bottom to allow electrolyte and gas flow. The glass fiber membrane was the same material as used above, only cut into a rectangle to cover the graphite bed fully. The seal between the BDD and plastic was created using three pieces of Parafilm M with a rectangular hole cut to fit the opening at the bottom of the reactor. The weight platform was a rectangular plastic piece that fit over the graphite press had a porthole for electrolyte addition. In order to ensure that the weight was centered on the graphite bed at all times, the weight platform had an additional circular plastic piece attached to it which had grooves which fit around two poles/retort stands, which served as guide rails. The counter electrode wire was fed out the top of the graphite press via a hole at the side of the press. The BDD was connected via a lead to the potentiostat using a piece of double-sided copper tape strongly adhered to the BDD.

Synthesis of electrochemically derived graphene oxide (EGO)

In both the smaller and larger version of the reactor, natural flake graphite (Sigma Aldrich Product Number 332461, particle size: +100 mesh) was poured through the opening at the top of the reactor (the amount varied and is specified in the text). The reactor was tapped several times to ensure the graphite was evenly distributed across the working electrode substrate. The glass fiber membrane separators and the 3D-printed graphite press were then placed atop the bed of graphite. Weight was then added to the top of the graphite press. For the smaller reactor, this consisted of roughly 0.5 kg (i.e. 0.3249 kg/cm^2), and for the larger reactor, 2.5 kg was added (0.2058 kg/cm^2). Note that in preliminary experiments, it was found that the reaction was not strongly dependent upon the weight, provided that the weight loading was less than 0.3249 kg/cm^2. The Pt wire counter electrode was cleaned before each experiment by first sonicating in acetone for 3 min and rinsing in ethanol and deionized water; then, the counter electrode was electrochemically cleaned. This cleaning was done in a three-electrode cell in 0.5 M H_2SO_4 and consisted of a constant +2 V for 2 minutes versus SCE, followed by cyclic voltammetry between -0.23 and 1.10 V versus SCE with a scan rate of 100 mV/s for 20 cycles (stopping at 1.1 V).

The sulfuric acid electrolyte (7.1-16 M, depending on the experimental condition, diluted with deionized water from 98% sulfuric acid purchased from ChemSupply (Gillman, SA, Australia)) was then pipetted into the reactor from a hole in the top. 3.6 mL of electrolyte was used for the smaller setup, and 28.4 mL was used for the larger setup. This volume ensured the graphite and Pt counter electrode were submerged in electrolyte. Before the start of the reaction, the graphite press was manually agitated to remove any entrapped air bubbles from the graphite bed. The working electrode substrate and the Pt wire counter electrode were connected to a Gamry Interface 1000 potentiostat (Gamry Instruments, Warminster, PA) in a two-electrode configuration, and a constant current

was then applied. After the experiment appeared to reach the final voltage plateau, it was allowed to continue to run until at least 60 coulombs of charge had been transferred from the graphite bed. This was to ensure that the final voltage plateau had in fact been reached and that the slope of the voltage curve had stabilized. Note that previous work in our lab has shown that once the reaction shifts to oxygen evolution and the voltage has reached its final plateau, the graphite experiences minimal additional functionalization.[1] When the graphite loading was 250 mg or more, the voltage curve did not plateau below 12 V (the voltage limit of the potentiostat), but rather began to rapidly rise at the end. In this case, the experiment was stopped when it was evident that the slope of the voltage curve was approaching vertical.

At the conclusion of the EGO synthesis, the reactor was disassembled. For the smaller setup, the graphite oxide was transferred to 125 mL of deionized water. For the larger ~ 4 g scale reactor, the product was first transferred into ~100 mL of 50 wt.% sulfuric acid to avoid excessive heat from acid dilution. The acid was then filtered off and the solids transferred into 1 L of deionized water. Note that in a control experiment, the product was transferred directly into deionized water; the XRD spectra did not change based on this difference in the washing procedure. The product was then stored in a refrigerator at 4 °C. The yield was found by pipetting up a known volume of the product solution, sonicating it for 5-10 minutes, forming a film via vacuum filtration, drying the film overnight in an 80°C oven in air, then quickly removing and weighing the freestanding film. The total mass of the product was calculated from this amount.

Additional details about the sample preparation used for characterization

To prepare the GO products for XRD characterization, most samples were cast into vacuum filtered membranes. For the EGO, unexfoliated product was placed in a vacuum filter cup and rinsed with deionized water several times. A small milligram-scale amount of the product was then sonicated in water for approximately 20 minutes. The solution was used to form a membrane via vacuum filtration. A roughly 13-mm-diameter disk, cut from the membrane, was adhered to a flat, zero background silicon wafer. The adhesion was accomplished by dropping a small, concentrated amount of the previously sonicated product onto the wafer, placing the membrane on top of the droplet, and allowing it to dry in ambient conditions. In some cases, the membrane was not dispersible in solvents (i.e. after 1 h thermal treatment), and so the membrane was carefully placed atop the silicon wafer. CGO XRD samples were prepared in the same manner, except that the material was centrifuge-washed as described in the main text (Synthesis of CGO section), and then used to form the vacuum filtered membrane.

For the study of the EGO mechanism, some XRD samples consisted of packed beds of graphite/GO. For XRD run on presonicated wet samples, the product was drained of excess liquid using vacuum filtration and then immediately packed into a shallow bed inside the cavity of an amorphous silicon wafer. For the presonication, dried samples, excess liquid was removed from the graphite oxide using vacuum filtration and the material dried at room temperature under vacuum for two days.

For X-ray photoelectron spectroscopy (XPS), the material was first subjected to high-speed centrifugation to fully separate it from the solvent. The centrifuge sediment was thoroughly mixed, drop cast onto a conductive Si/SiO_2 wafer, and dried overnight under vacuum at room temperature. The remaining product was freeze-dried in preparation for further characterization. For the SEM, AFM, and single-flake Raman analysis, the freeze-dried product was resuspended in DMF at a concentration of 0.1 mg/mL. To exfoliate the EGO fully, the product was sonicated for 10 min, then low speed shear mixed for 10 min, sonicated for 10 min, then shear mixed again for 10 min. Shear mixing was performed with a Dragonlab D-500 homogenizer (2-cm-diameter mixing head with vertical slotted screen) operated at its lowest speed setting. Finally, EGO was spin coated onto a conductive Si/SiO_2 wafer (for SEM and AFM) or a 300 nm wet thermal oxide silicon wafer (for single flake Raman spectroscopy).

Supplementary Figures

A. Graphite foil based EGO forming process[2-3]

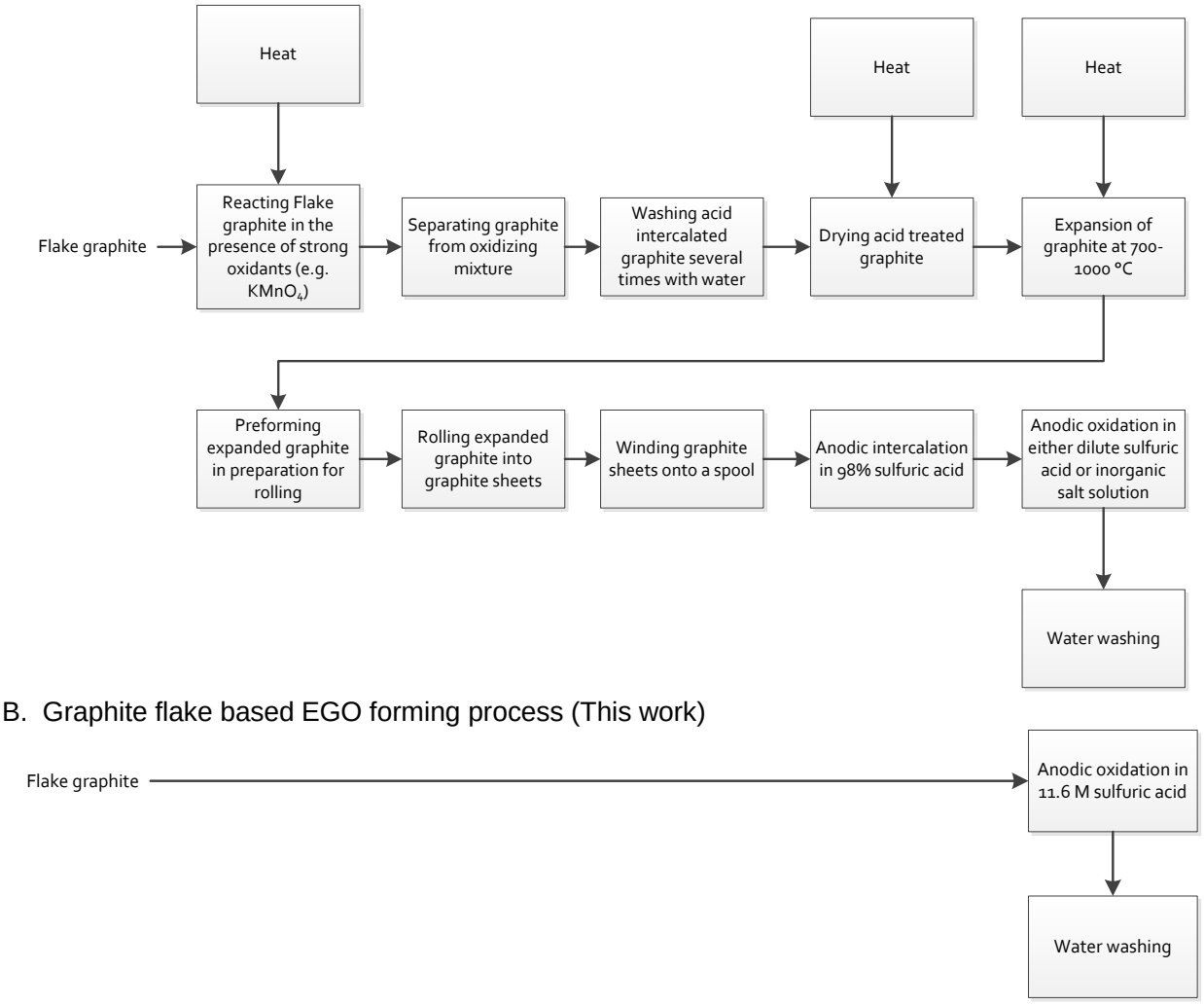

Figure S1. Process flow diagrams for EGO synthesis which uses graphite foil as its direct input (a) versus the current work, which uses graphite flakes directly (b). For (a), the steps for the synthesis of acid intercalated graphite were adapted from ref. [4], the steps required to make graphite sheets/graphite foil were adapted from ref. [5], and the process for two-step EGO oxidation of graphite foil was adapted from refs. [2-3]. N.b. graphite rod can also be used to synthesize EGO. However, this process does not start with mined flake graphite, but rather amorphous carbon (namely, calcined petroleum coke) which is later graphitized.[6-7] Therefore, the process is not directly comparable to ours. However, graphite rod manufacture is a complex, multi-day process requiring high (>1000 °C) temperatures, complexity which is captured in its price, shown in Table S1.

Figure S2. Small-scale electrochemical cell used to oxidize 40-750 mg flake graphite.

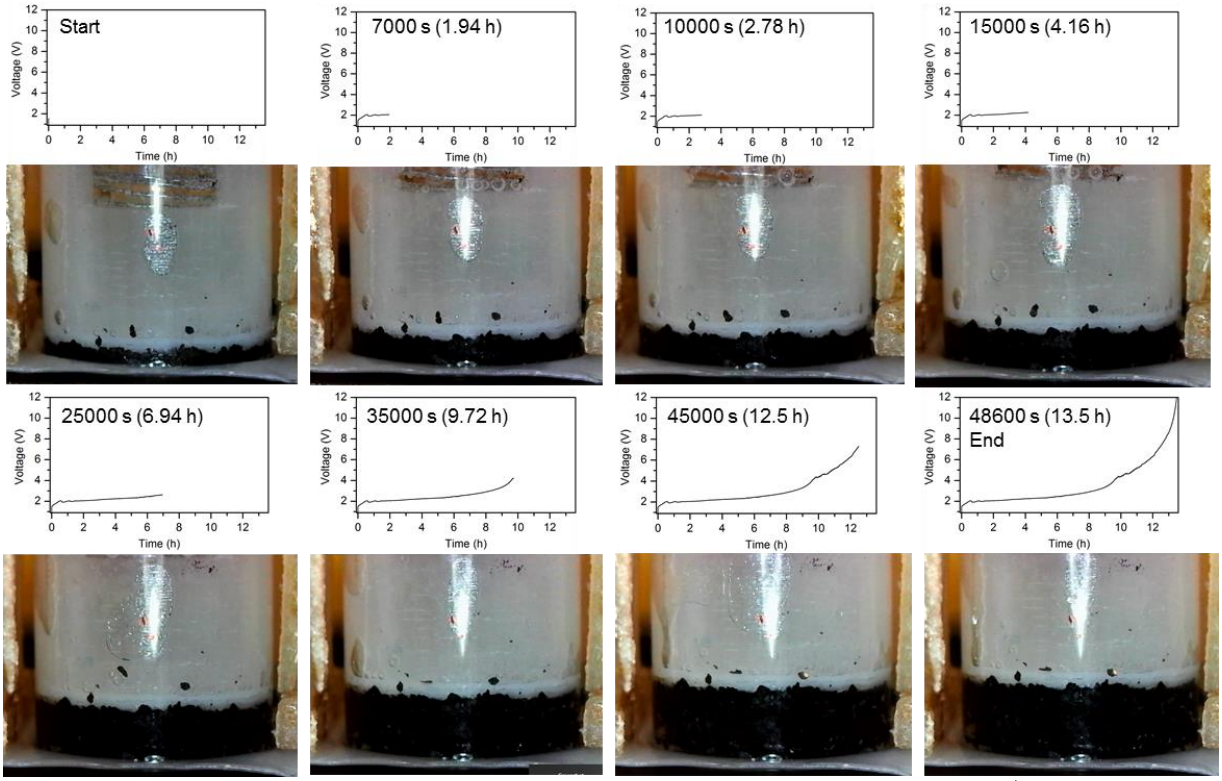

Figure S3. Photographs of the graphite bed expanding throughout the reaction with accompanying charging curves (whole cell voltage versus time). 250 mg of graphite was used as the starting material, with an 11.6 M sulfuric acid electrolyte and 24 mA constant current. The starting height of the bed was approximately 1.4 mm, and the final height was 4.70 mm. In later photographs, bubbles can be seen emerging from the sides of the beds. Video recordings of this experiment showed that the bubbling rate increased around 29000 s (8 h, around 2.91 V), as the voltage began to rise from its initial plateau, ascribed to oxygen evolution from the graphite bed.

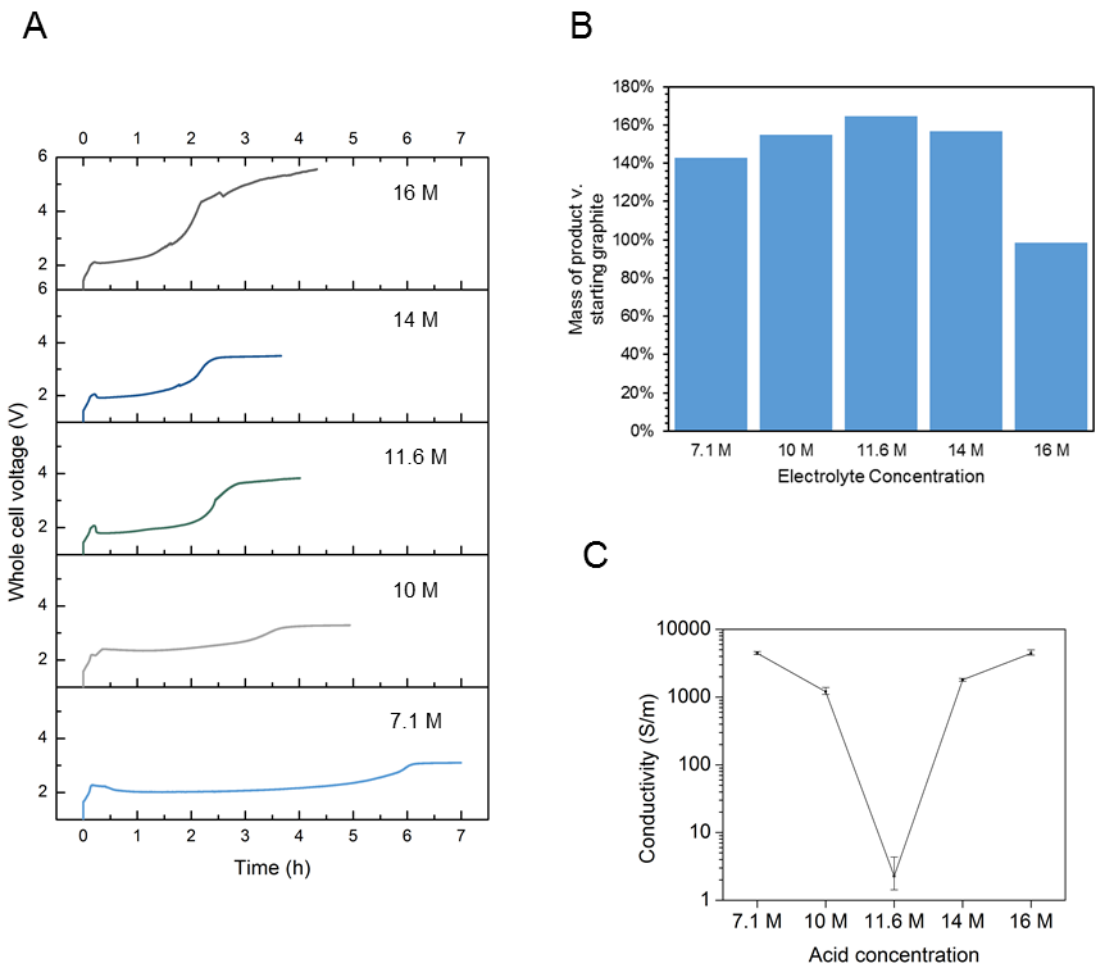

Figure S4. The effect of electrolyte acid concentration on the reaction.(a) Galvanostatic charging curves for the reaction at different electrolyte concentrations, with constant starting graphite (40 mg) and current (16 mA). (b) Mass gain as a function of electrolyte concentration. (c) Film conductivity as a function of electrolyte concentration. Error bars cover the interquartile range.

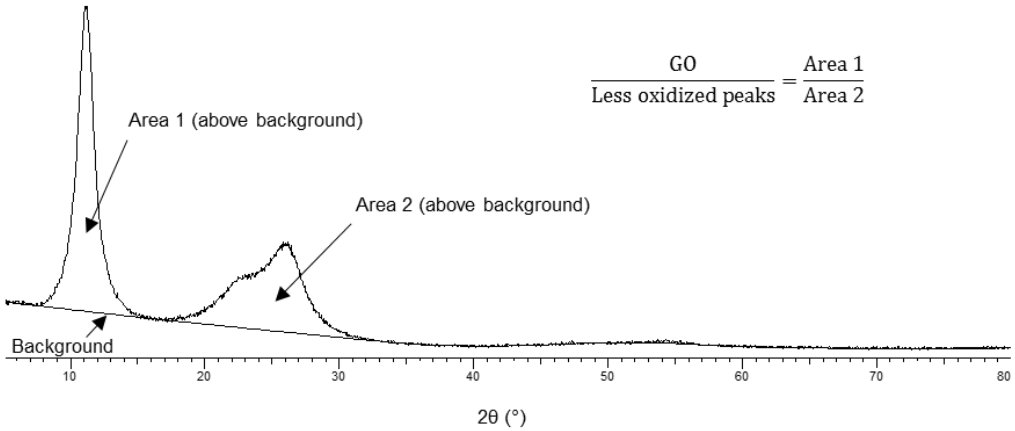

Figure S5. Calculation of the ratio of primary graphite oxide peak v. peaks corresponding to less oxidized components.This ratio provides a measure of the amount of graphite oxide in each sample relative to less oxidized components (although we note that because the intensity of each peak may change at a different rate with changes in the concentration of the underlying species, the ratio is only a correlation). Data shown is for the 10 M sulfuric acid, 16 mA current, 40 mg starting graphite condition.

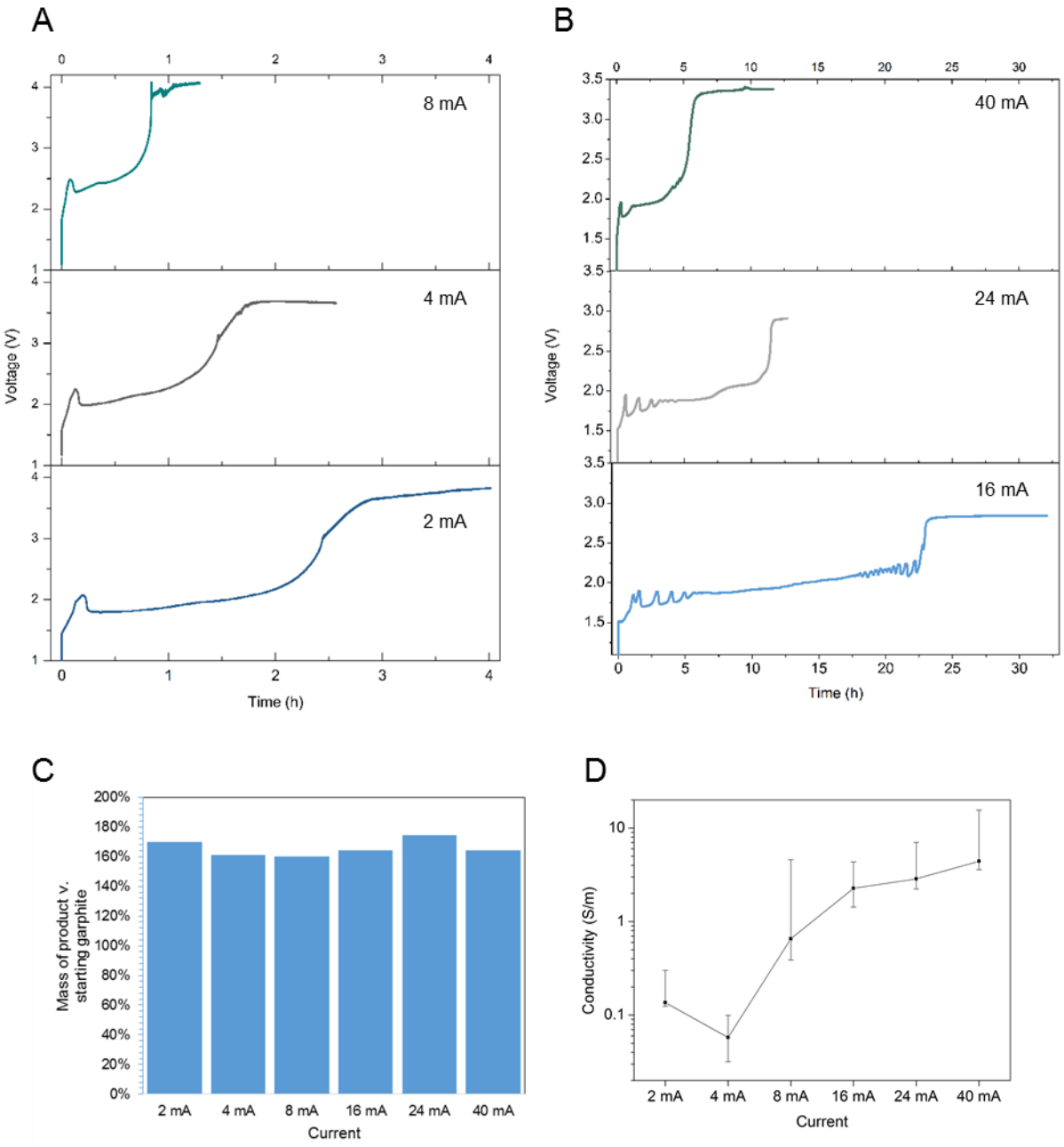

Figure S6. The effect of the applied current on the reaction.(a-b) Galvanostatic charging curves for the reaction at different current values, with the starting graphite (40 mg) and electrolyte (11.6 M sulfuric acid) constant. (c) Mass gain as a function of applied current. (d) Film conductivity as a function of applied current. Error bars cover the interquartile range.

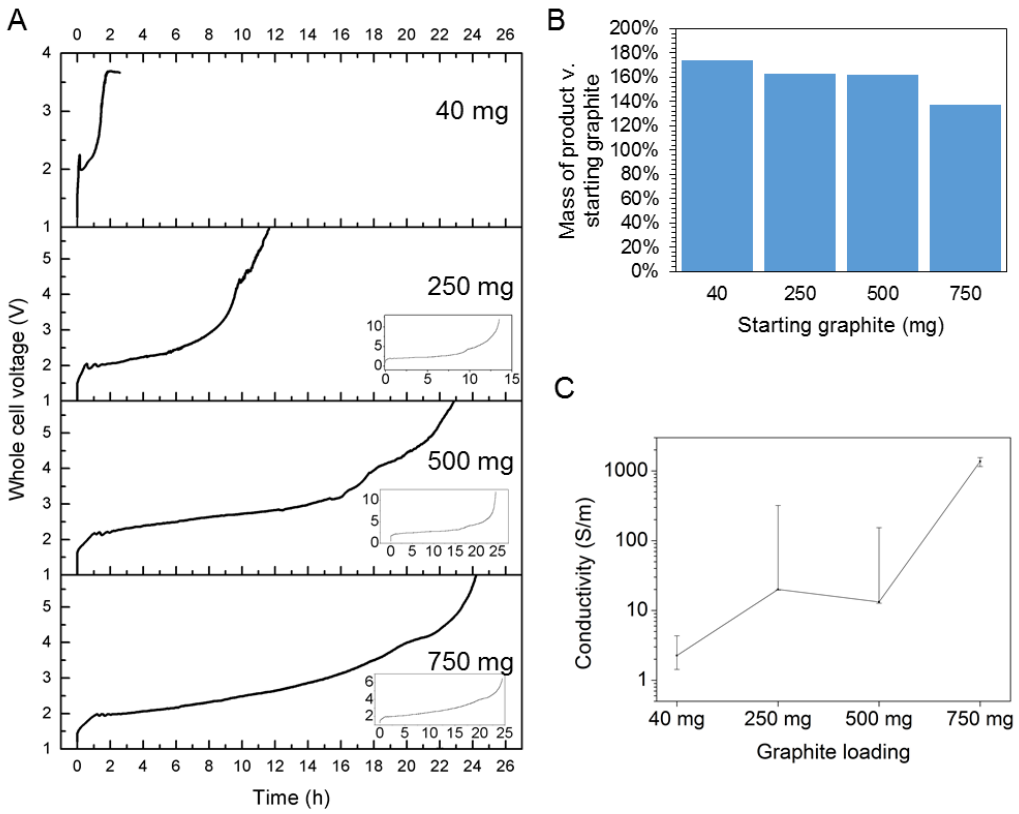

Figure S7. The effect of the graphite loading on the reaction.(a) Galvanostatic charging curves for the reaction at different starting graphite amounts. Inset shows complete charging curve. (b) Mass gain as a function of the starting graphite amount. (c) Film conductivity as a function of the starting graphite amount. Error bars cover the interquartile range.

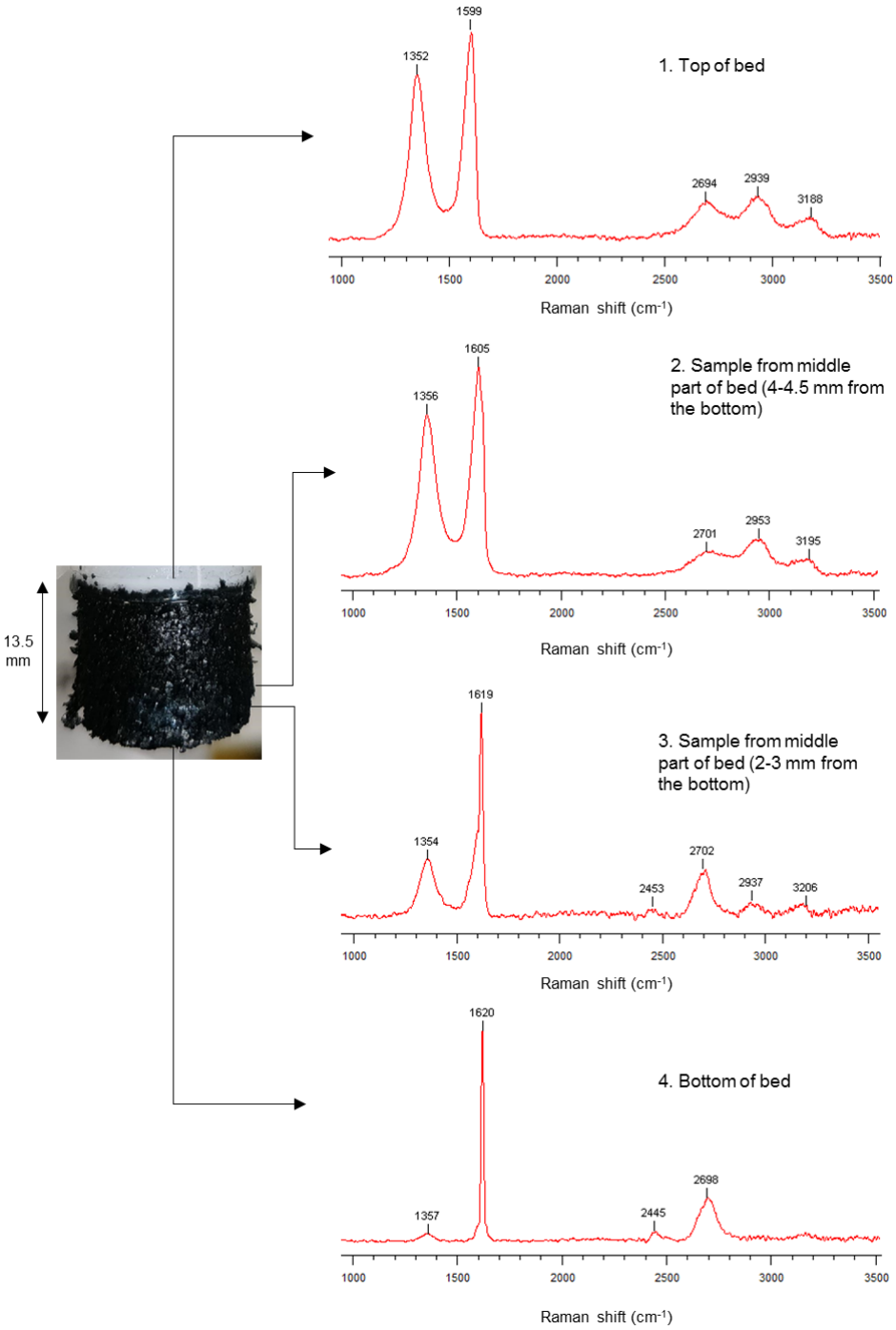

Figure S8. Raman spectra of samples taken from different locations along the height of the bed from the 750 mg starting graphite experiment (24 mA current, 11.6 M sulfuric acid electrolyte). At the end of the reaction, the packed bed was carefully removed from the reactor, and tweezers were used to take samples from various points. These samples were immediately probed with Raman spectroscopy while still in the experimental electrolyte. The top two samples (samples 1-2) appear to be GO, the bottom sample (sample 4) exhibits the E_{2g} band at 1620 cm^{-1} (but no $E_{2g'}$ band) characteristic of a stage V or higher graphite intercalation compound (GIC),[8] and sample 3 appears to be a mixture of the GO and the GIC.

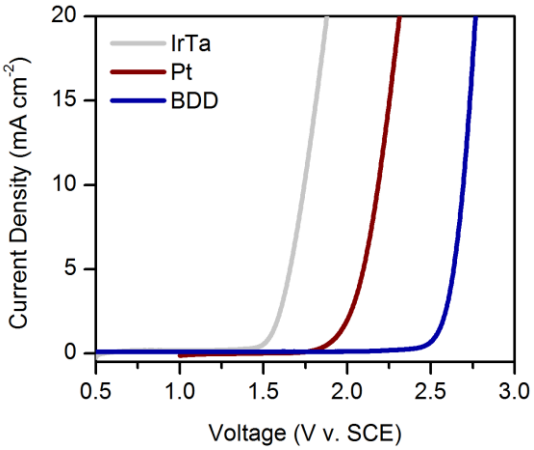

Figure S9. Linear sweep voltammetry in the experimental electrolyte, 11.6 M sulfuric acid, using three different working electrodes, iridium tantalum mixed metal oxide (IrTa), platinum (Pt), or boron-doped diamond (BDD).

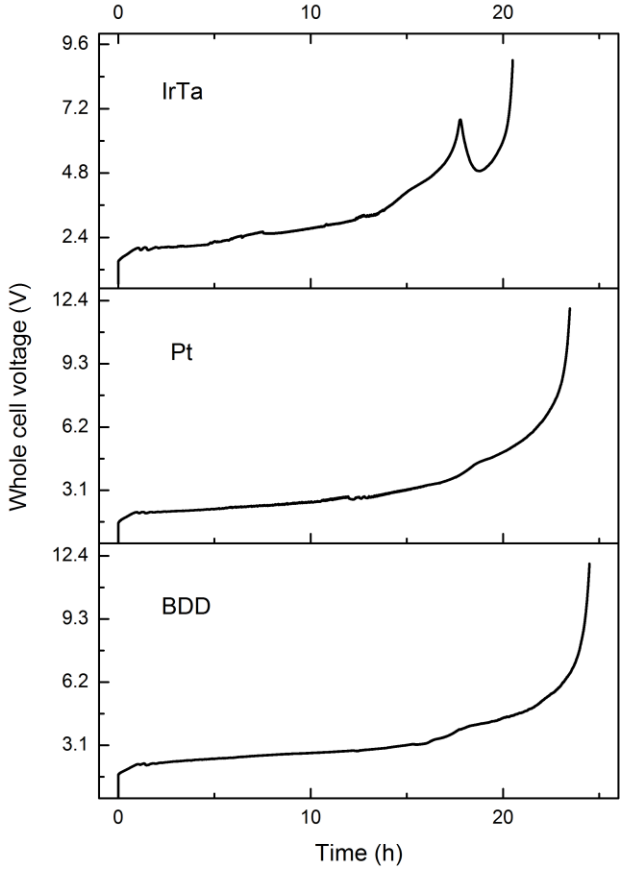

Figure S10. Charging curves for the 500 mg scale reaction (11.6 M sulfuric acid electrolyte, 24 mA current) using three different working electrodes, iridium tantalum mixed metal oxide (IrTa), platinum (Pt), or boron-doped diamond (BDD).

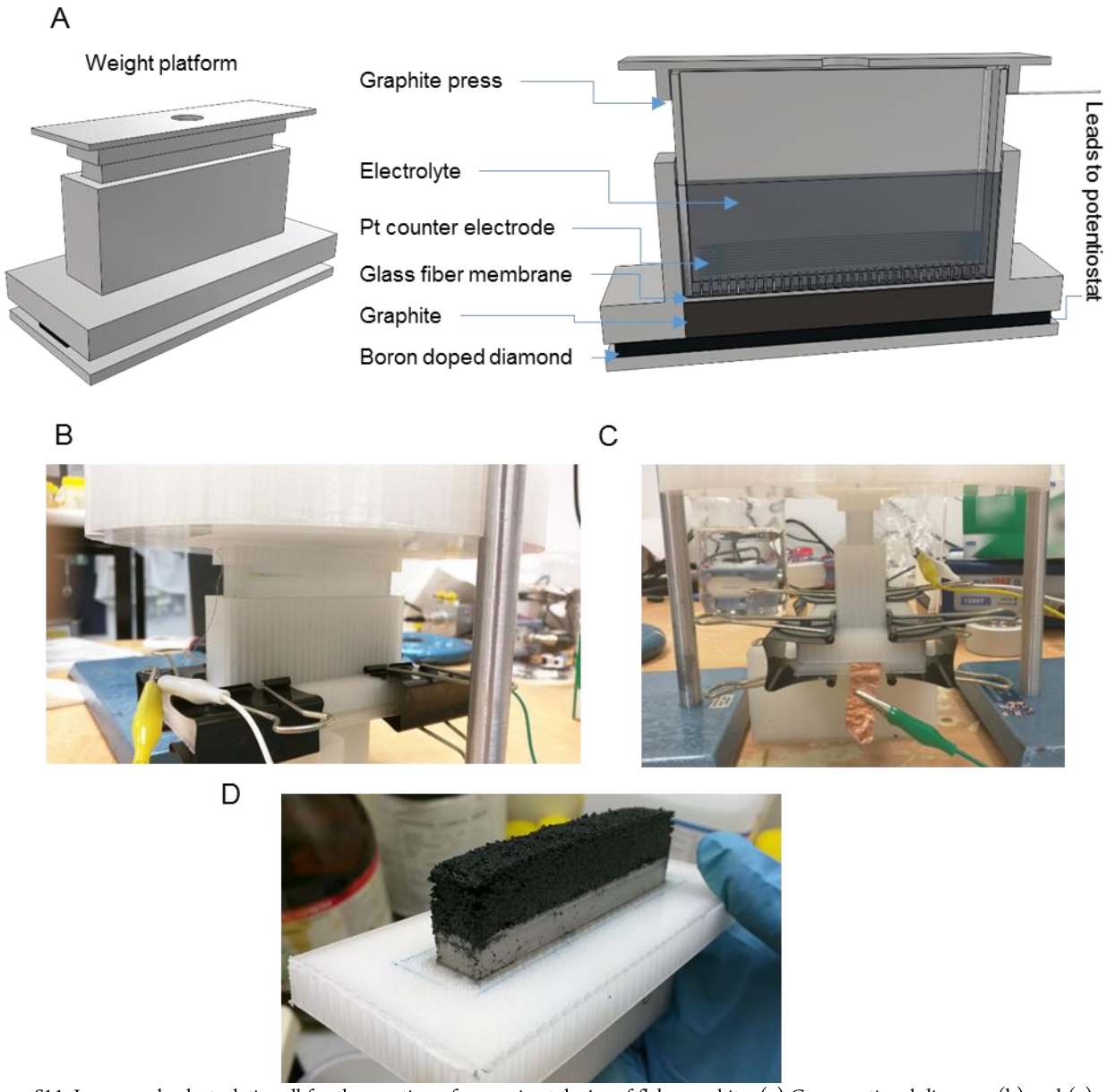

Figure S11. Larger scale electrolytic cell for the reaction of approximately 4 g of flake graphite. (a) Cross sectional diagram. (b) and (c) Different views of the reactor. (d) The graphite oxide product at the end of the reaction; the boron-doped diamond working electrode substrate was removed, the reactor was inverted, and the product was pressed upwards using the plastic press.

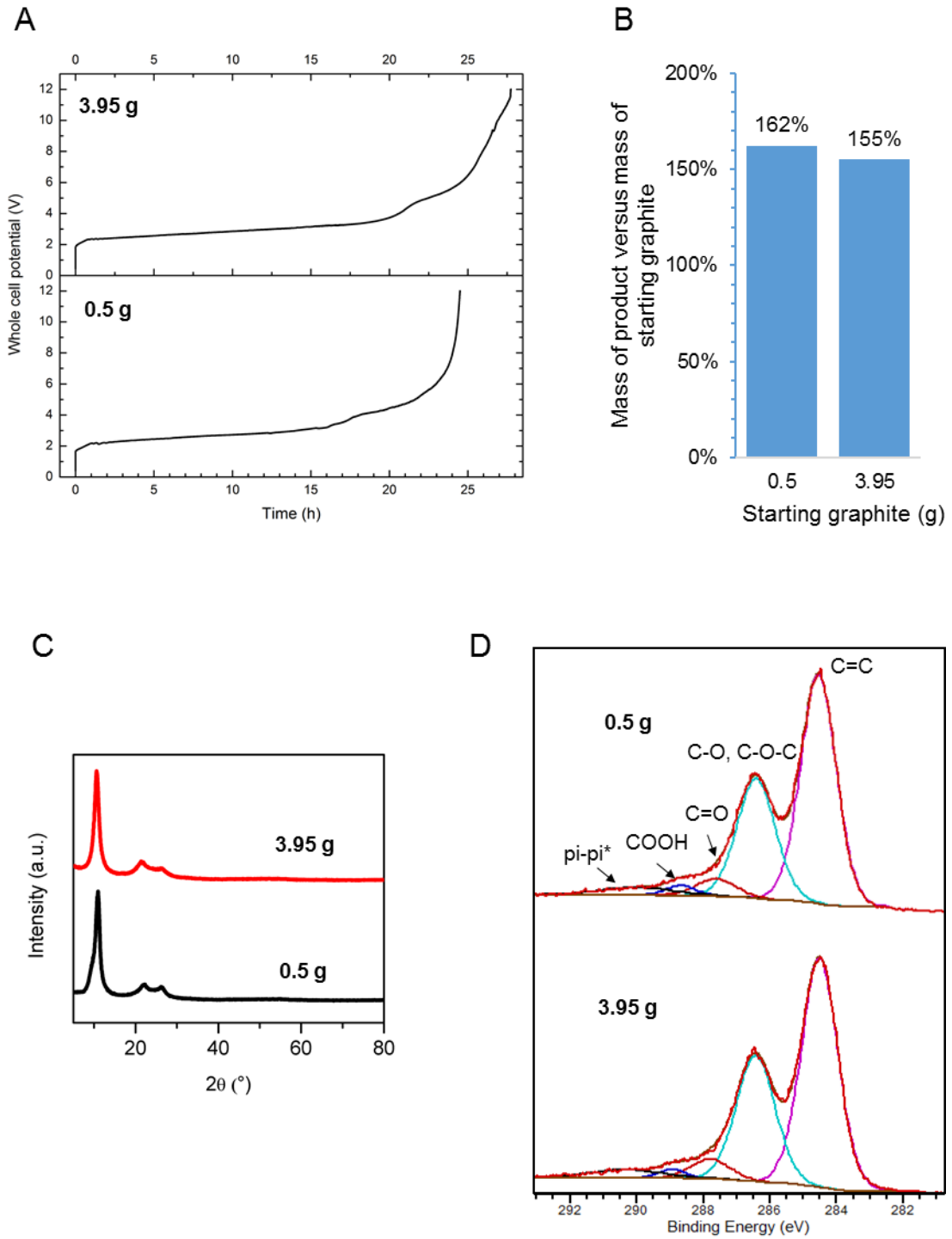

Figure S12. Characterization of the 500 mg reaction in the smaller, tubular reactor versus the scaled 3.95 g reaction in the larger, rectangular reactor. (a) Galvanostatic charging curves. (b) Mass change of the graphite after the reaction. (c) XRD diffractograms. (d) XPS C 1s spectra with deconvoluted components. Quantification of the component areas is shown in Table S7.

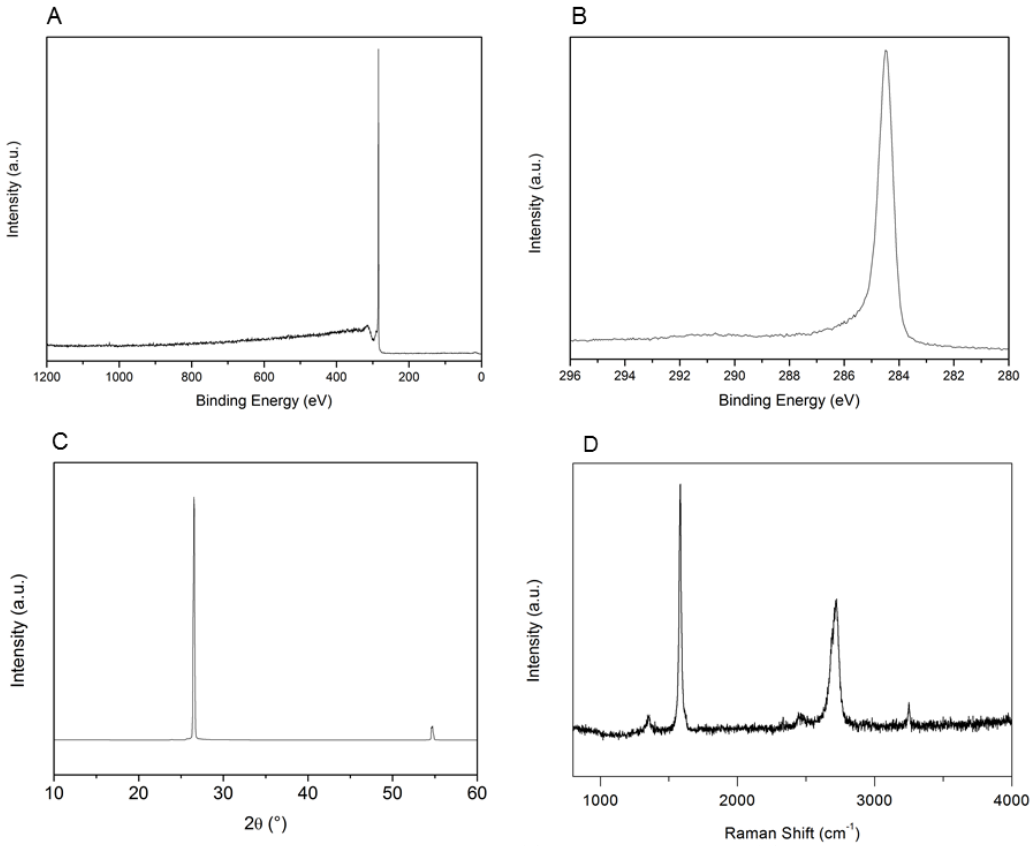

Figure S13. Natural flake graphite precursor used for EGO synthesis: (a) XPS survey spectrum, (b) XPS C 1s high resolution spectrum, (c) XRD diffractogram, and (d) Raman spectrum.

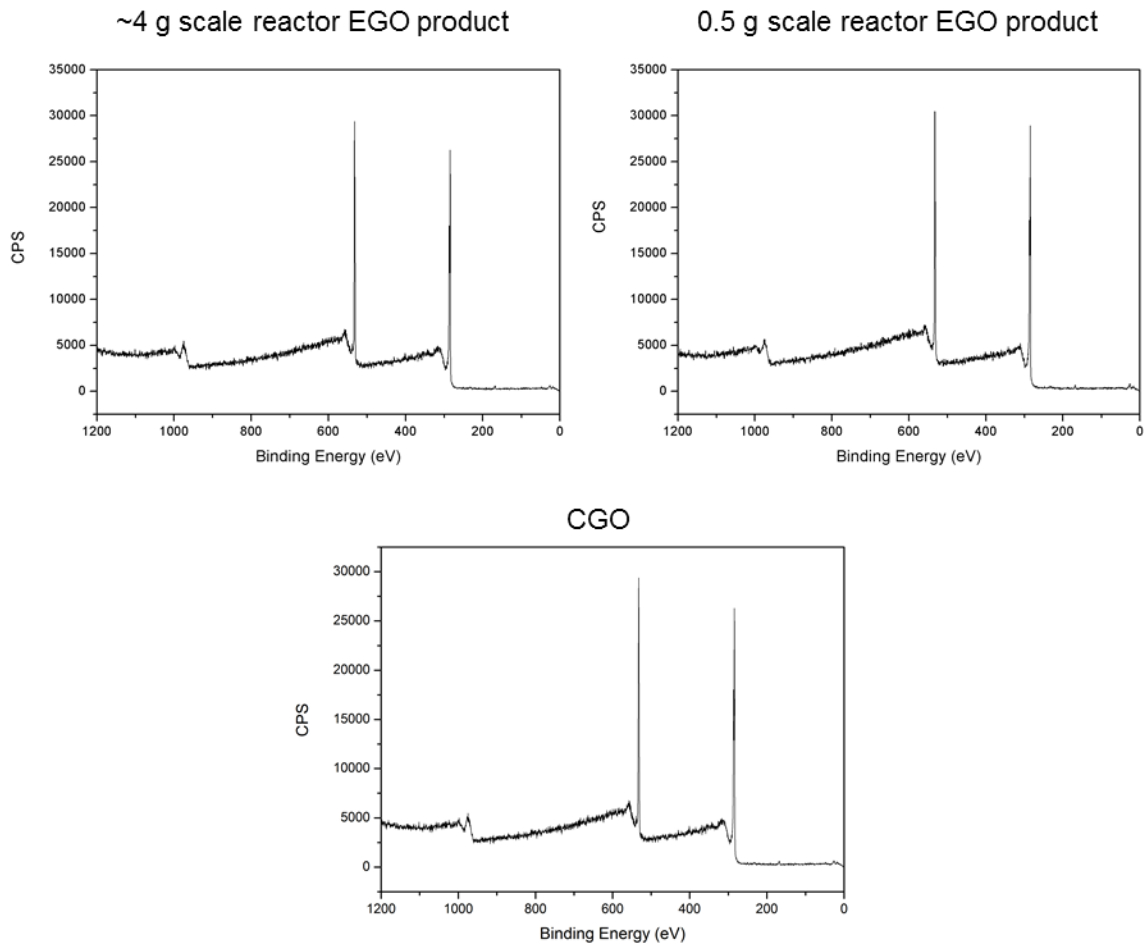

Figure S14. XPS survey spectra for the as prepared larger-scale EGO products and CGO. Y-axis units are arbitrary.

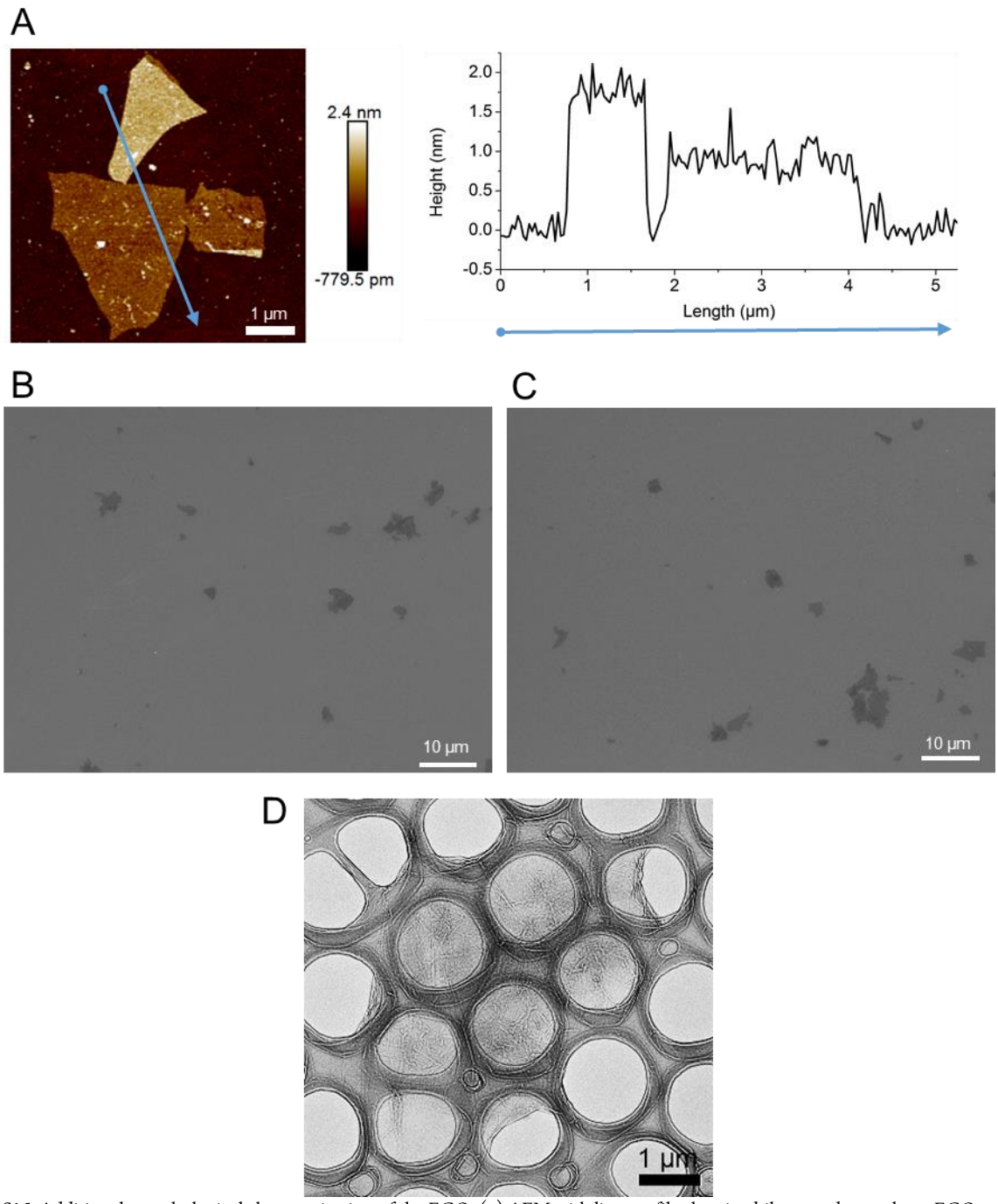

Figure S15. Additional morphological characterization of the EGO. (a) AFM with line profile showing bilayer and monolayer EGO and (b, c) SEM micrographs of the ~4 g scale EGO product dispersed in DMF and spin coated onto a Si/SiO_2 wafer. Several of these type of micrographs were statistically analyzed to generate flake size statistics. (d) TEM micrograph of an EGO flake.

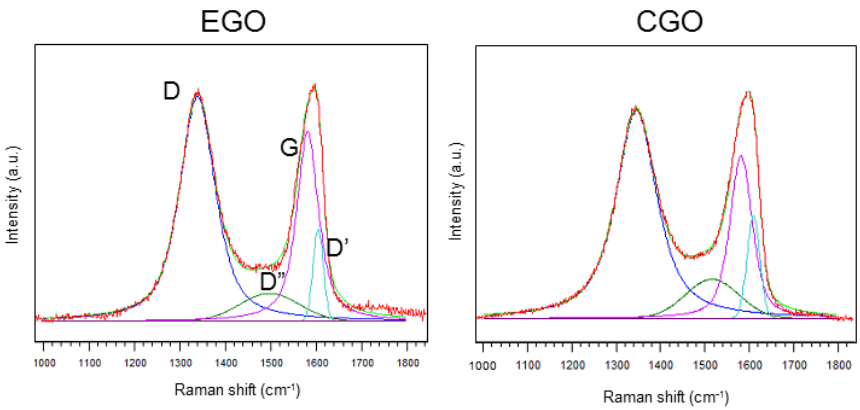

Figure S16. Deconvolution of the Raman spectra of electrochemically derived graphene oxide (EGO) versus chemically derived graphene oxide (CGO) films with peak assignments.

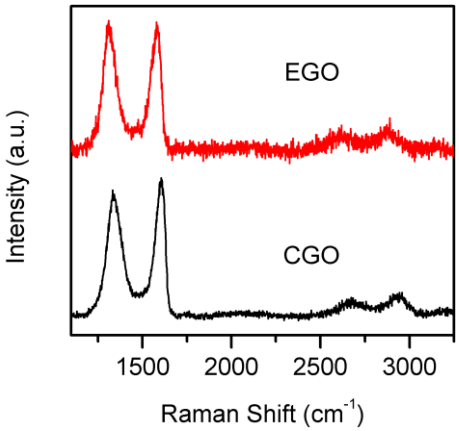

Figure S17. Raman spectra acquired on single or few layer flakes of electrochemically derived graphene oxide (EGO) or chemically derived graphene oxide (CGO) spin coated onto a wet thermal oxide silicon wafer. The flakes were selected based on their optical contrast under the light microscope, with very faint flakes assumed to be few layer graphene.

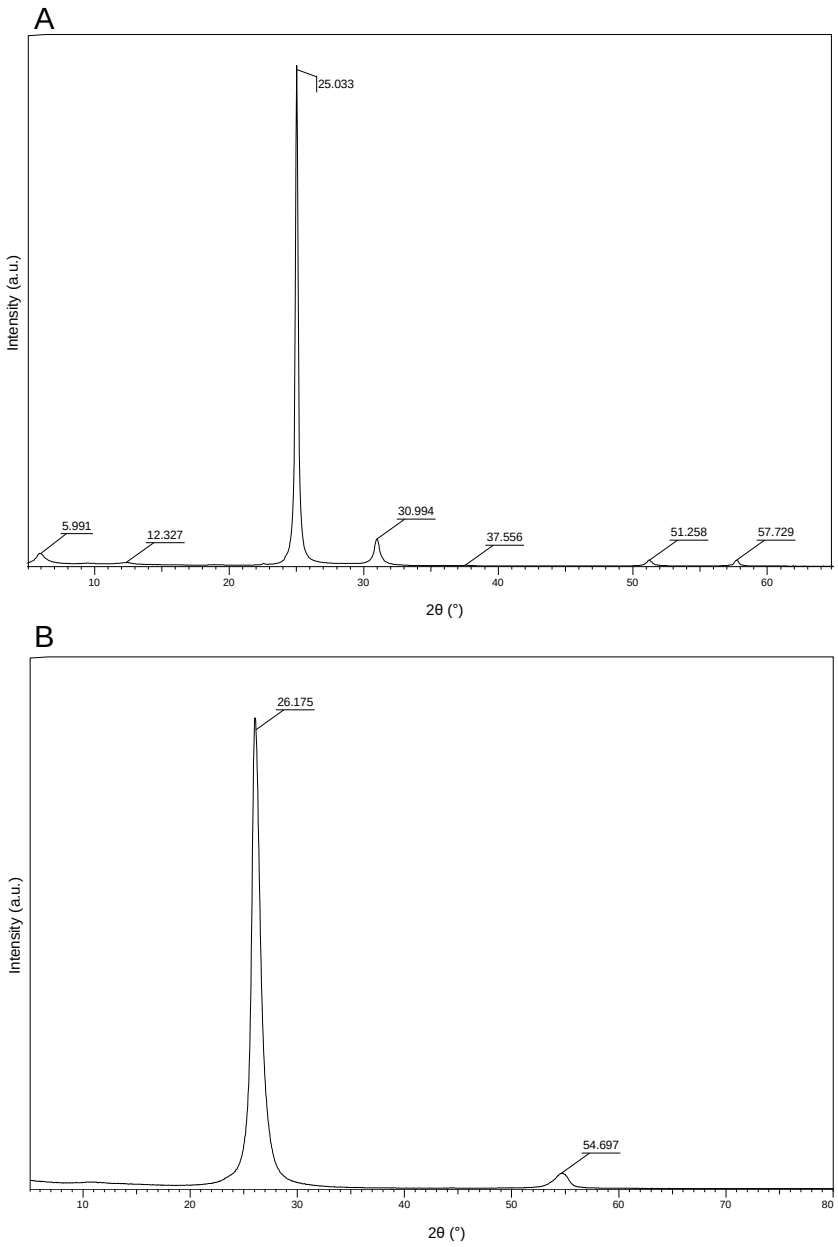

Figure S18. XRD diffractograms for the bottom component of the partially reacted packed bed, magnified and peak labelled. (a) The product just removed from the reactor characterized in the experimental electrolyte (11.6 M sulfuric acid). (b) The product after being washed in water and dried overnight.

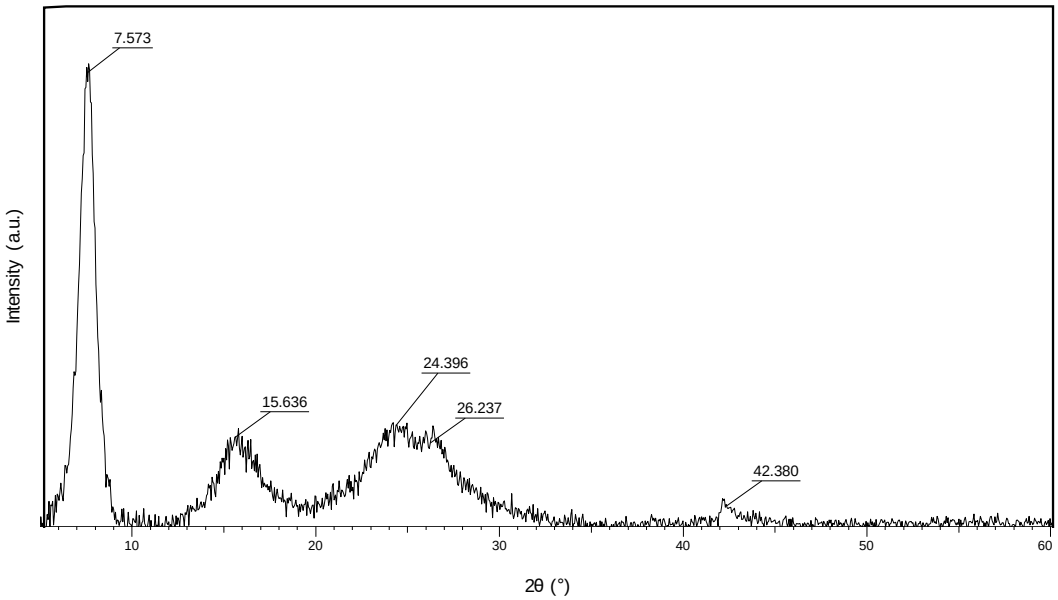

Figure S19. XRD diffractogram of acetone washed and dried top component of the partially reacted packed bed; the product has been washed and soaked in solvent overnight then allowed to dry for two days.

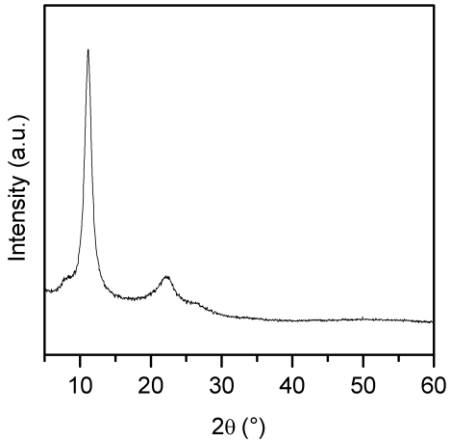

Figure S20. XRD diffractogram of the post-sonication product isolated from the top component of the partially reacted packed bed; the product has been washed and soaked in water overnight, sonicated in water, then vacuum filtered to form a membrane and dried overnight.

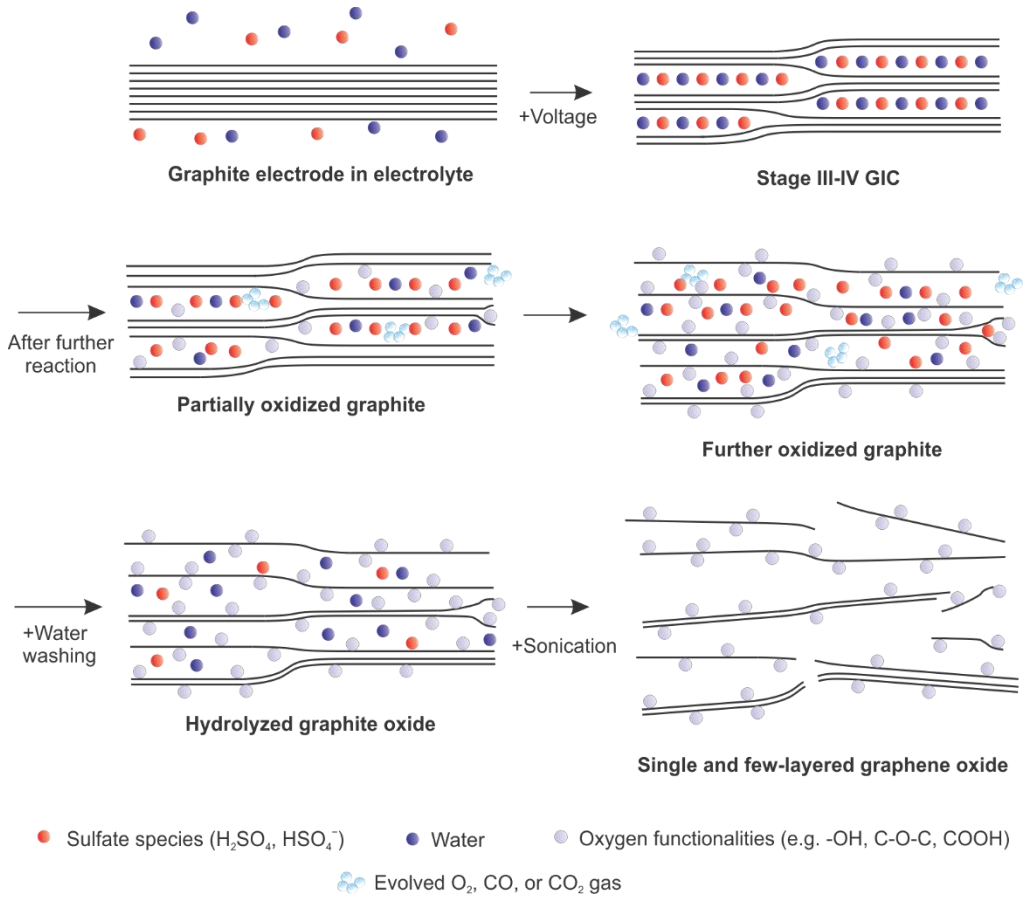

Figure S21. Proposed mechanism for the electrochemical formation of graphene oxide from flake graphite. Graphite is first intercalated to form a Stage III-IV graphite intercalation compound (GIC). Subsequently, graphite flakes are oxidized by water or oxygen radical species under prolonged anodic conditions. As the reaction progresses, intercalant further intrudes into the graphite gallery and additional parts of the graphite are oxidized. After the reaction, the product is washed, hydrolyzing sulfates and possibly reacting with the graphite further. Finally, with sonication in water or organic solvent, the graphite oxide is separated into few-layered graphene oxide.

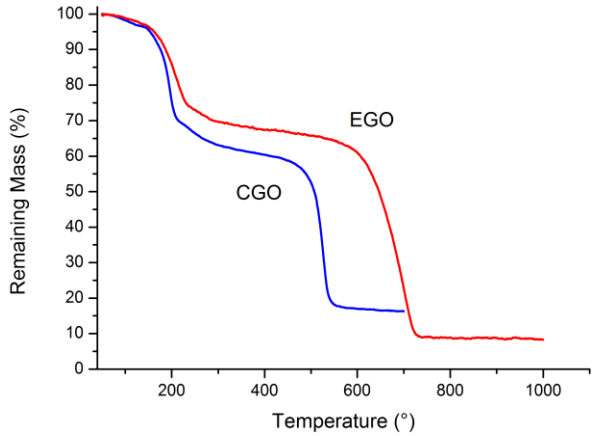

Figure S22. TGA study of CGO and EGO membranes in a 20% oxygen, 80% argon atmosphere. The temperature was initially held at 50 °C for 2.5 hours, and then increased by 5 °C/min.

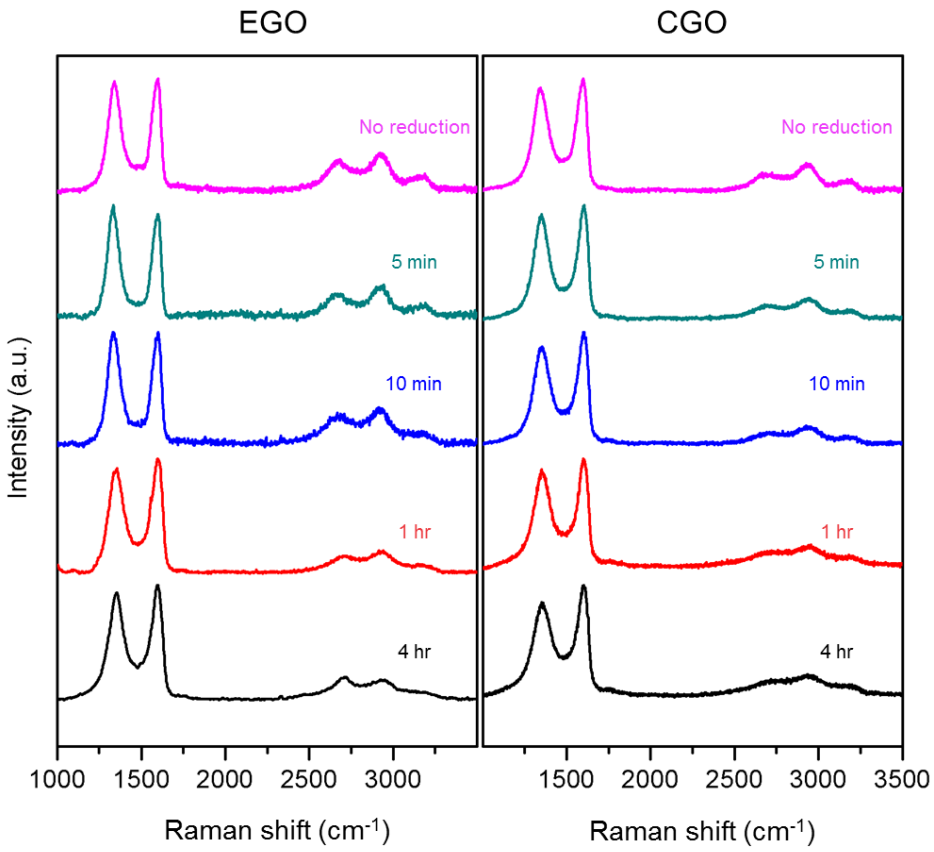

Figure S23. Evolution of the Raman spectra of electrochemically derived graphene oxide (EGO) versus chemically derived graphene oxide (CGO) films during thermal treatment for various times in a 200 °C oven in air.

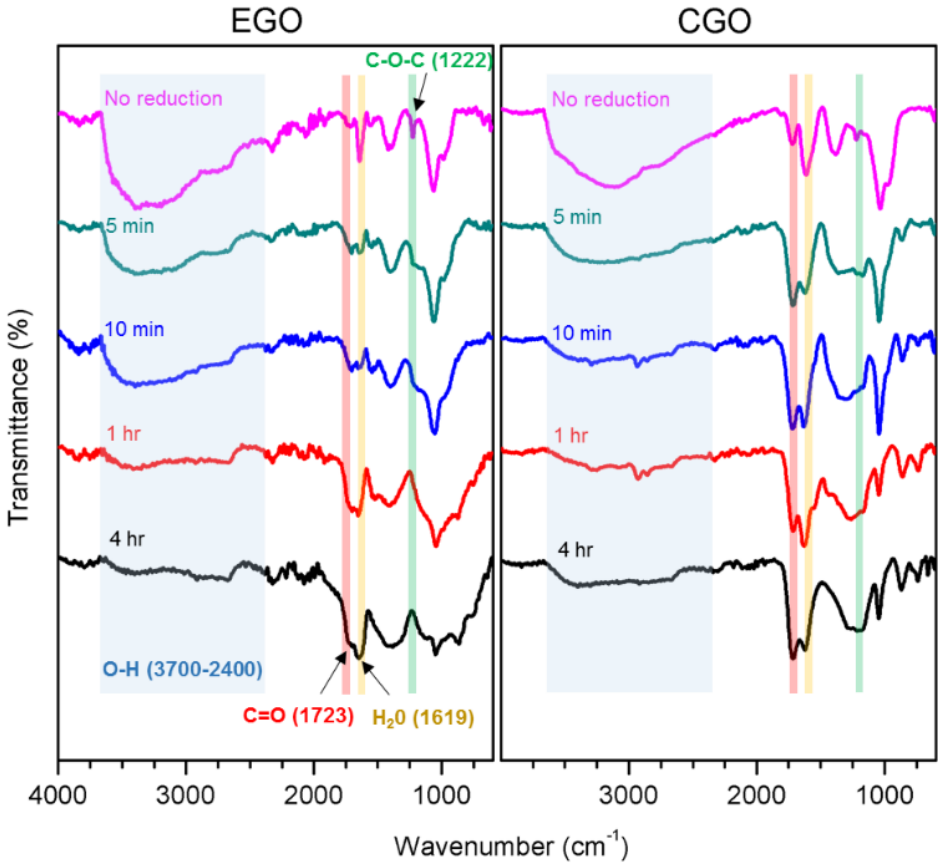

Figure S24. Evolution of the FTIR spectra of electrochemically derived graphene oxide (EGO) versus chemically derived graphene oxide (CGO) films during thermal treatment for various times in a 200 °C oven in air. Peaks associated with the presence of various oxygen functional groups are highlighted.

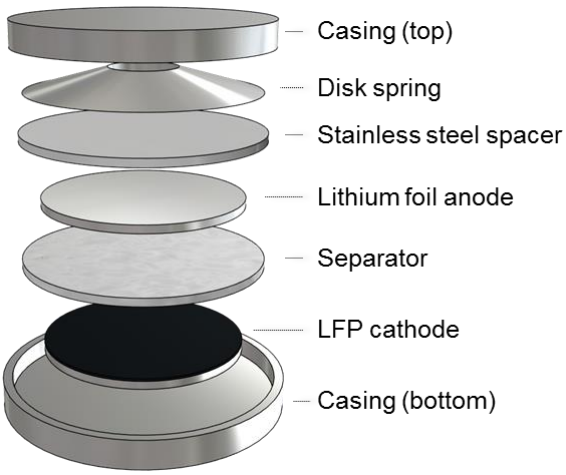

Figure S25. Exploded view of coin cell setup.

3D models used for the 3D printing of the packed bed reactors

The original STL files associated with the 3D models are available upon request.

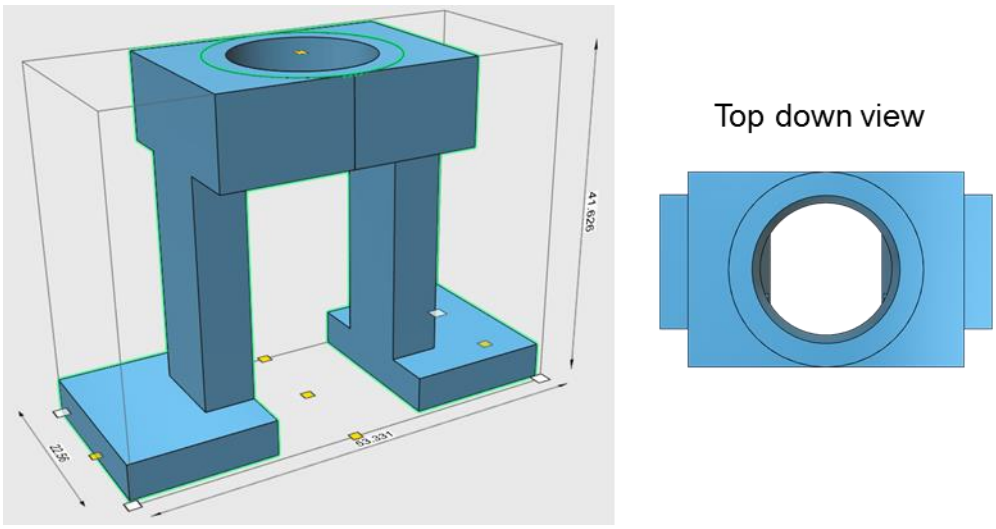

Figure S26. 3D model used to print the glass tube holder and clamping flanges used to build the smaller scale reactor.

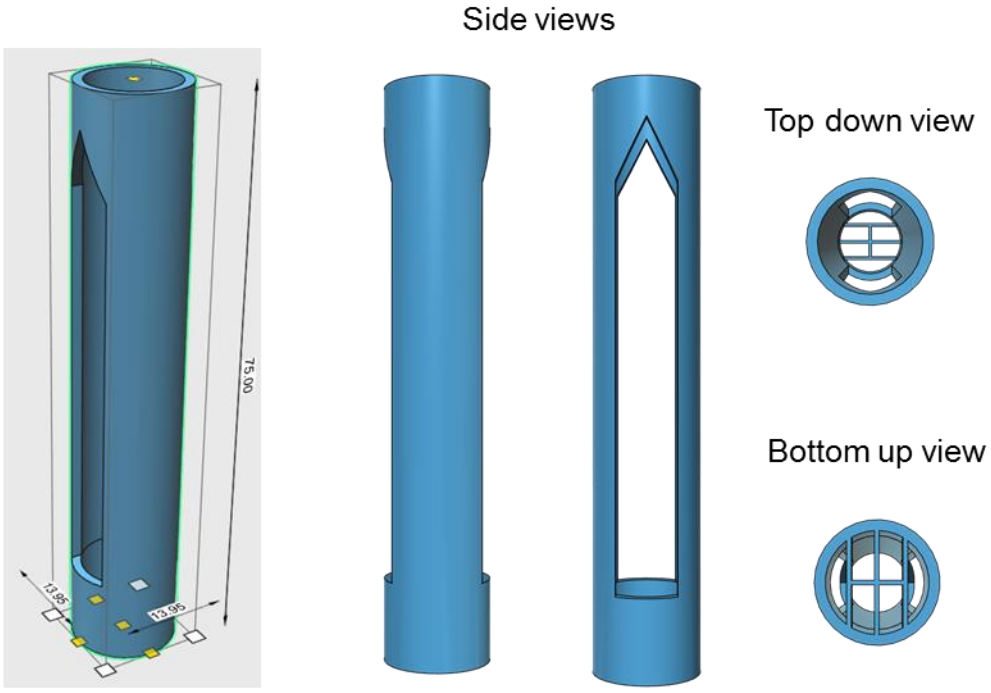

Figure S27. 3D model used to print the graphite press used in the smaller scale reactor. Dimensions are in mm.

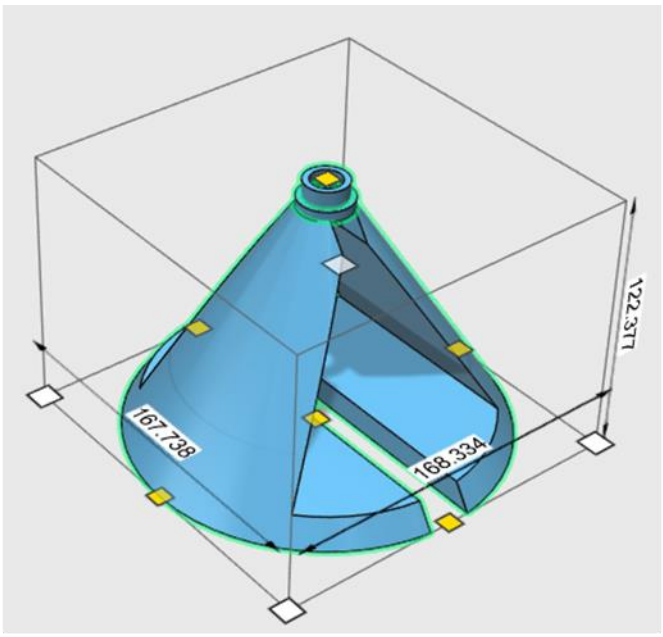

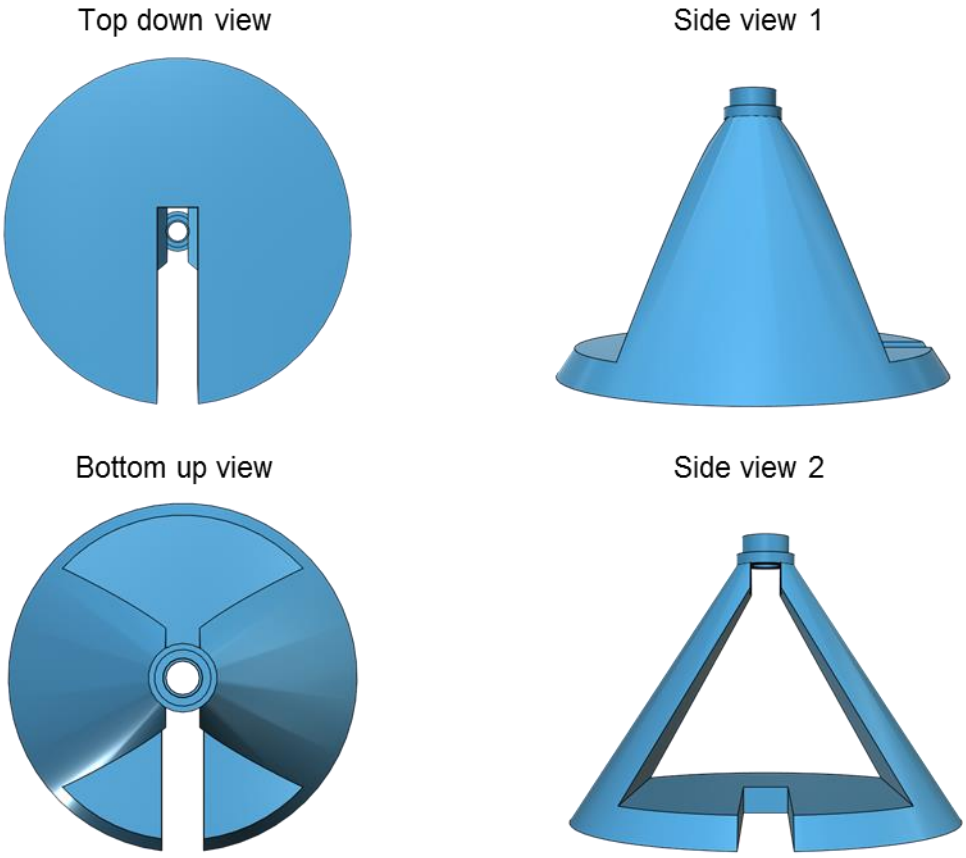

Figure S28. 3D model used to print the weight platform used in the smaller scale reactor. The bottom of this part was glued to the top of the graphite press shown in Figure S27 to form a single piece. Dimensions are in mm.

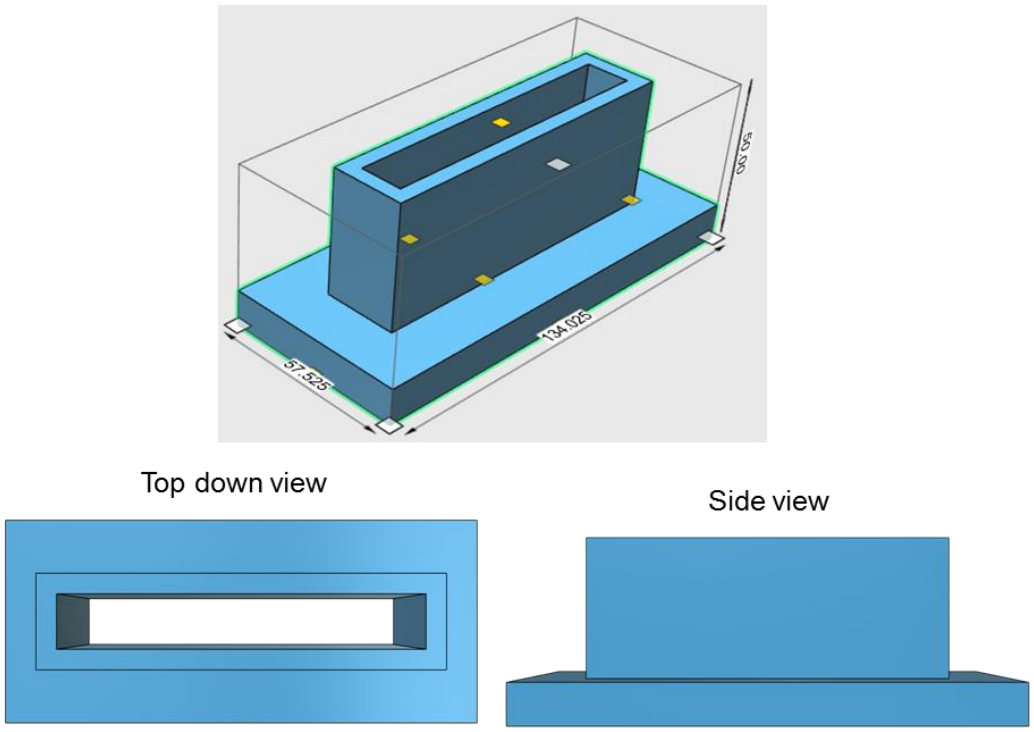

Figure S29. 3D model used to print the larger scale reactor. Dimensions are in mm.

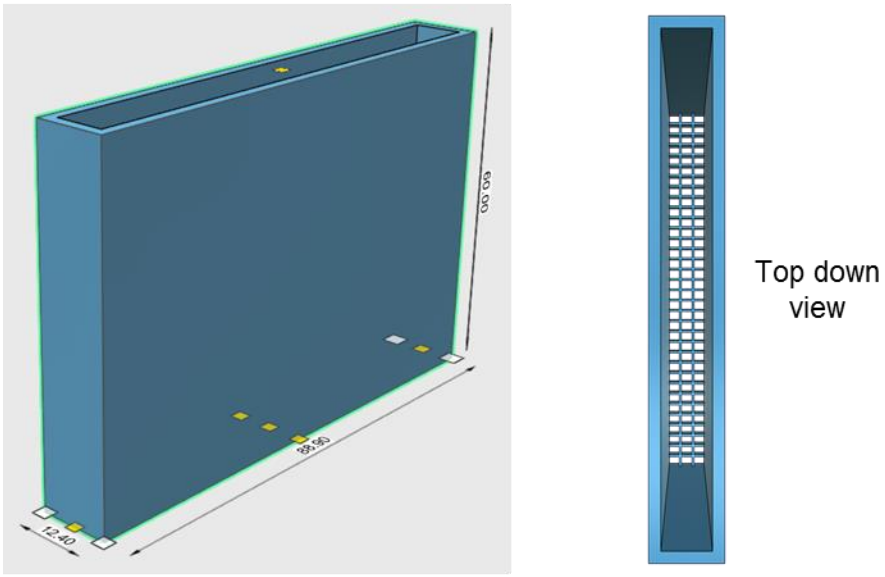

Figure S30. 3D model used to print the graphite press used in larger scale reactor. Dimensions are in mm.

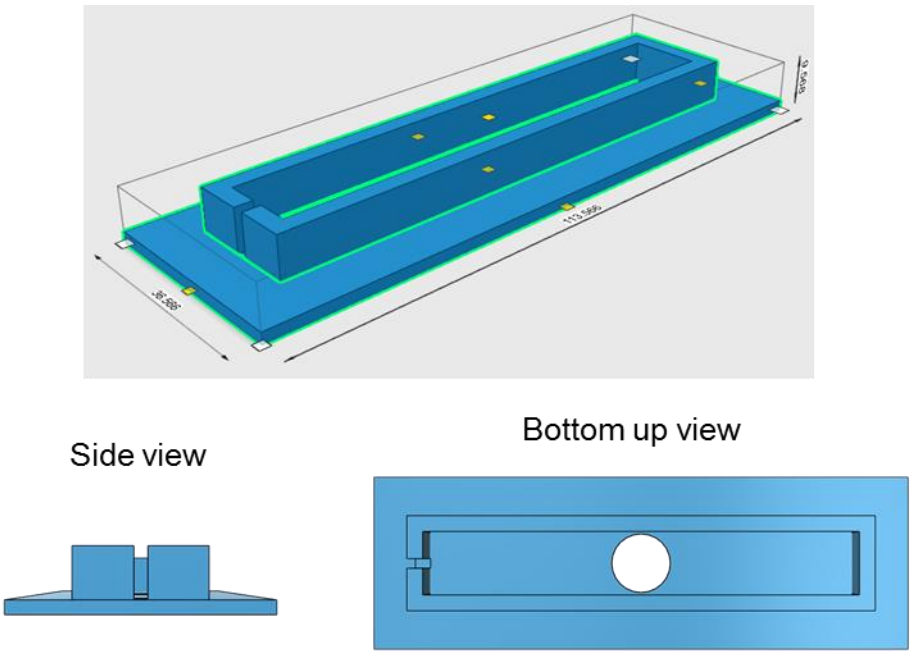

Figure S31. 3D model used to print the graphite press cap used in the larger scale reactor. Dimensions are in mm.

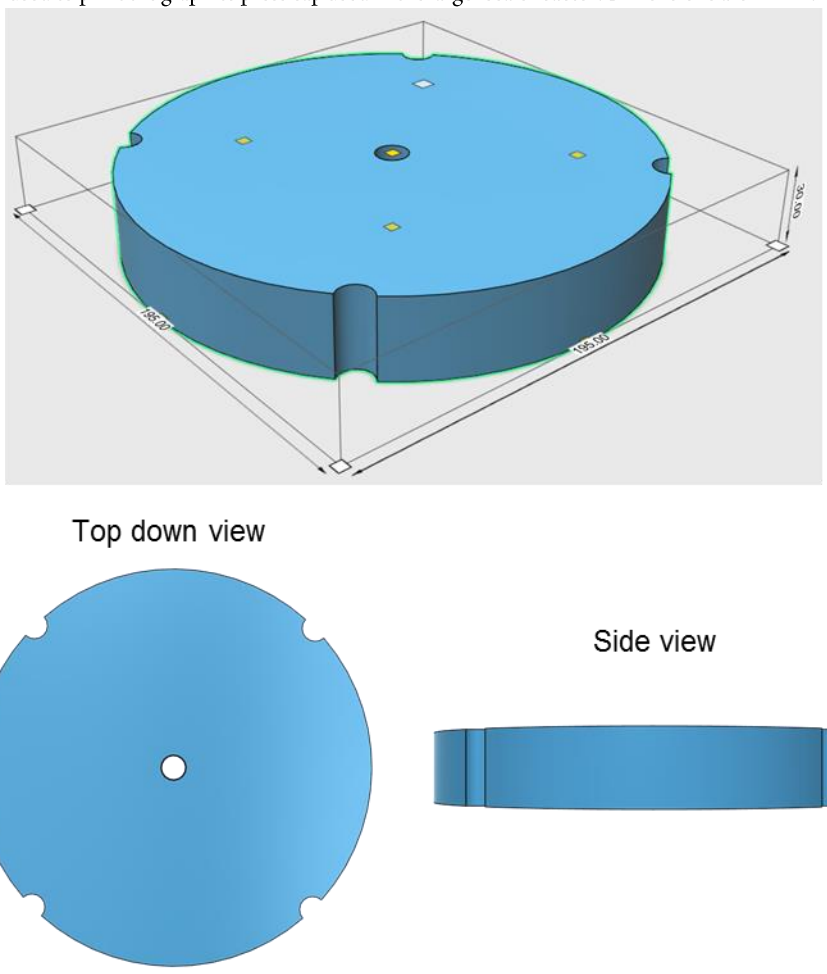

Figure S32. 3D model used to print the weight platform used in the larger scale reactor. Dimensions are in mm.

Supplementary Tables

Table S1. Comparison of the cost of graphite precursors for EGO synthesis

Graphite source	Cost (USD)	Source
Solid packed graphite (e.g. graphite rod or graphite electrode)	$10,064 per metric ton in 2018 for industrial sized graphite electrodes	[9]
Graphite foil (also known as flexible graphite sheet)*	$0.1 per square meter of 0.5 mm thick graphite foil, $25,000-$100,000 per metric ton	[10]
Flake graphite	$1,000-1,300 per metric ton for Chinese graphite delivered to Europe, 94-97% C +80 mesh size	[11]

*Note that graphite foil is a high-end, processed form of graphite, rather than a commodity input. Thus, unlike flake graphite and solid graphite electrodes, it is often sold by the square meter and its price is not tracked by common industry trade magazines/databases.

Table S2. Review of all reported electrochemically produced graphene or graphite oxide studies in the academic literature in the graphene era (i.e. post-Geim and Novoselov, 2004)[12-14]

Reference	Starting graphite	Reactor configuration	Electrolyte	Oxygen content (atom % or C/O ratio)	% of product retained for analysis*
This work	Natural graphite flakes	Packed bed	11.6 M sulfuric acid	20%	100%
Pei et al. 2018[2]	Graphite foil	Parallel plate reactor	Concentrated sulfuric acid, followed by 50 wt.% sulfuric acid	C/O = 1.7	Product weighs 96% of starting graphite weight
Cao et al. 2017[3]	Graphite foil	Parallel plate reactor	Concentrated sulfuric acid, followed by 0.1 M ammonium sulfate	17.7%	71%
Tian et al. 2017[1]	Natural graphite flakes compressed into a disk	Graphite disk between two parallel plates	4.6-11.6 M perchloric acid (11.6 being the optimized concentration)	25%	100%
Gurzęda et al 2017[15]	Flake graphite enclosed in a Pt mesh	Parallel plate reactor	11 M sulfuric acid	23.1%	100%**
Gurzęda et al. 2016[16]	Flake graphite enclosed in a Pt mesh	Parallel plate reactor	8 M perchloric acid	9.25%	100%**
Parvez et al. 2016[17]	Graphite rod	Parallel plate reactor	1 M ammonium sulfate	28.3%	80%
Markovic et al. 2016[18]	Graphite rod or HOPG	Parallel plate reactor	Ammonium persulfate	22-25%	76% (for a graphite rod starting material), 42% (for HOPG)
Yu et al. 2015[19]	Natural graphite flakes	Stirred graphite flakes	1 M sulfuric acid in saturated ammonium sulfate aqueous solution	21%	Product weighs 37.6% of starting graphite weight
Rao et al. 2015[20]	Graphite rod	Parallel plate reactor	Glycine in dilute sulfuric acid	11%	2.2 g/L

Abdelkader et al. 2014[21]	Unclear from text (presumably graphite rod)	Parallel plate reactor	0.2 M sodium citrate	C/O = 7.6	80-88% (as a proportion of the mass removed from the anode)
Liu et al. 2013[22]	Pencil core	Parallel plate reactor	1 M phosphoric acid	Not reported	100%†
Singh et al. 2012[23]	Pencil core	Parallel plate reactor	Triethyl sulfonium bis(trifluoromethyl sulfonyl) imide ionic liquid	Not reported	Not reported

* Defined as the mass of the product retained after separation (via centrifugation, sedimentation, etc.) as a percentage of the total mass of the product after the reaction, including unreacted graphite. Where this value was not reported, another measure of yield is shown, if available.

** Graphite oxide rather than graphene oxide produced. Reduced graphene oxide was produced after thermal treatment.

Table S3. Electrochemical oxidation of 3.9 g flake graphite using the newly developed method using the large setup

Preparation step	**Time required**
Reactor setup	15 minutes
Electrochemical synthesis	27.5 hours
Reactor disassembly and water washing with vacuum filtration, sonication and centrifugation	3 hours
Total time	**~32 hours**

Table S4. Chemical oxidation of 1 g flake graphite using a two-step modified Hummer's method*

Preparation step	**Time required**
Pre-oxidation treatment**	
Reactor setup	15 minutes
Synthesis of graphite intercalation compound (GIC) in concentrated H_2SO_4 and $KMnO_4$	15 minutes
Separating graphite from acid mixture; washing with water to form pre-oxidised graphite	15 minutes
Drying at elevated temperature (90 °C)	4 hours-overnight
GO synthesis	
Reactor setup	15 minutes
$KMnO_4$ addition in an ice bath	1 hour
Reaction at 45 °C	4 hours
Cooling the reaction and holding in ice bath	2 hours
H_2O_2, HCl addition and overnight sedimentation	18 hours
Water washing with six rounds of centrifugation (20 minutes per round)	2 hours
Total time	**≥32 hours**

* The procedure outlined reflects the methods used to produce chemically derived graphene oxide (CGO) in this study.

** In our study, preoxidised graphite for CGO synthesis was sourced from Asbury Graphite Mills. To provide a comparison with the EGO process, the minimal time required for graphite pre-oxidation is provided based on a standard method.[4]

Table S5. Two component fitted statistics for the D and G peaks of as prepared EGO and CGO

Sample	Component Name	Peak center	Full width at half maximum (cm^{-1})	Intensity (a.u.)
EGO	D	1341.82	94.15	19865
EGO	G	1588.19	64.67	20124
CGO	D	1349.31	116.35	13549
CGO	G	1589.19	75.25	14192

Table S6. Four component fitted statistics for the D and G peaks of EGO and CGO.

Peak	Statistic	CGO	EGO
D	FWHM (cm^{-1})	111	94
	Intensity (a.u.)	13591	19592
	Center (cm^{-1})	1346	1340
	% Gaussian	26	34
	Area (a.u.)	2169400	2570680
D"	FWHM (cm^{-1})	143	155
	Intensity (a.u.)	2560	2427
	Center (cm^{-1})	1518	1499
	% Gaussian	100	100
	Area (a.u.)	389792	400009
G	FWHM (cm^{-1})	60	57
	Intensity (a.u.)	10651	16539
	Center (cm^{-1})	1583	1583
	% Gaussian	44	23
	Area (a.u.)	865716	1377330
D'	FWHM (cm^{-1})	35	27
	Intensity (a.u.)	6706	7998
	Center (cm^{-1})	1611	1607
	% Gaussian	100	100
	Area (a.u.)	246680	228521

* Note that a D* component was not needed to fit the curve well, as previously found by López-Díaz et al. for CGO synthesized from natural flake graphite[24]

Table S7. Deconvolution results for XPS analyses of larger scale EGO experiments and chemically derived graphene oxide (CGO)

	CGO		**EGO, ~4 g scale**		**EGO, 0.5 g scale**	
	Position	Atom %	Position	Atom %	Position	Atom %
C=C	284.46	44.8%	284.51	58.6%	284.51	59.3%
C-O, C-O-C	286.34	37.6%	286.39	34.2%	286.38	33.3%
C=O	287.79	11.4%	287.25	5.5%	287.59	5.1%
COOH	289.03	6.2%	288.60	1.8%	288.65	2.3%
π-π^*			290.39		290.00	

Table S8. Conductivity and mass loss of EGO and CGO membranes as a function of thermal treatment time at 200° C in air

	Mean conductivity (S/m)		**Mass remaining (%)**	
Thermal treatment time	EGO	CGO	EGO	CGO
Initial	45.912	0.005	100	100
5 min	1268.5	8.7	86	84
10 min	2561.9	23.8	85	69
1 hour	17882.5	877.1	68	55
4 hours	16491.2	494.1	64	55

Supplementary Notes

Supplementary Note 1: Additional notes on the effect of acid concentration

Measurement of the mass of the final product versus the mass of the starting graphite (the 'yield' shown in **Error! Reference source not found.** and Figure S4b) supports the conclusion that the 11.6 M condition was most oxidized. A maximum yield of 160% was recorded for the 11.6 M acid condition. This mass increase is driven by increased oxygen addition to the carbon lattice.

Note that previous studies,[1, 25-26] including work in our lab,[1] on anodic graphite oxidation in mineral acids have found there is an optimal balance between the amount of acid versus water in the electrolyte. It appears that when the acid concentration is greater than optimal, there is insufficient water to act as oxidant, limiting the graphite oxide forming reaction. If the acid concentration is too low, however, there is insufficient acid intercalation to catalyze oxidation of the basal plane.

The higher acid concentration was chosen not only to optimize extent of oxidation, but also to control the reaction time. Examination of the charging curves (shown in Figure S4a), shows that total time required for the reaction to reach its final voltage plateau decreases as the acid concentration increases, possibly due to increased current efficiency for graphite oxidation over water splitting.

Supplementary Note 2: Additional notes on the effect of graphite loading

The total reaction time, as measured by the time taken for the voltage to reach its final plateau or achieve a near vertical slope , was roughly proportional to the starting mass when the mass was less than 500 mg (see charging curves in Figure S7). However, when the starting graphite was increased to 750 mg, the charging time did not increase markedly. This suggests that less charge was transferred away from the graphite lattice per unit mass, and that the graphite was less oxidized. This is further supported by the fact that the mass recovered with respect to the starting graphite was significantly less in the 750 mg condition, 137%, as compared to the 500 mg condition, 162%.

Supplementary Note 3: Additional notes on the mechanism and role of water

In the mechanism illustrated in Figure S21, water acts as an oxidant to functionalize the graphitic carbon. This mechanism initially was proposed in early work[26] and supported by recent ^{18}O isotropic tracing experiments showing the source of oxygen in sulfuric acid-based EGO is water.[2] Note that the precise mechanism involved in transfer of oxygen from water to graphite has still not be fully elucidated in the literature. On the one hand, there may be an acid hydrolysis of the GIC by water/OH^- anions, eventually leading to covalent bond formation.[26-27] However, it has also been suggested that hydroxyl or other oxygen radicals formed during the process of water electrolysis can act as oxidants, oxidizing the graphite instead of proceeding to form O_2 gas.[2, 28-30] It is likely the reaction scheme is complex and that both of these pathways play a role.

Interestingly, while recent work has suggested that low stage intercalation compounds (i.e. near stage I) are important for EGO formation,[1-31-3] in our model, single-layer EGO can be produced from higher stage GICs. Thus, the initial degree of acid intercalation does not determine oxygen functionalization of the basal plane. Oxygen functionalization, along with oxygen evolution, may work in tandem with acid intercalation to open the graphite gallery and allow diffusion of oxidants in.

Supporting Information References

(1) Tian, Z.; Yu, P.; Lowe, S. E.; Pandolfo, A. G.; Gengenbach, T. R.; Nairn, K. M.; Song, J.; Wang, X.; Zhong, Y. L.; Li, D., Facile Electrochemical Approach for the Production of Graphite Oxide with Tunable Chemistry. *Carbon* **2017**, *112*, 185-191.
(2) Pei, S.; Wei, Q.; Huang, K.; Cheng, H.-M.; Ren, W., Green Synthesis of Graphene Oxide By seconds Timescale Water Electrolytic Oxidation. *Nat. Commun.* **2018**, *9*, 145.
(3) Cao, J.; He, P.; Mohammed, M. A.; Zhao, X.; Young, R. J.; Derby, B.; Kinloch, I. A.; Dryfe, R. A. W., Two-Step Electrochemical Intercalation and Oxidation of Graphite for the Mass Production of Graphene Oxide. *J. Am. Chem. Soc.* **2017**, *139*, 17446-17456.
(4) Sorokina, N.; Khaskov, M.; Avdeev, V.; Nikol'Skaya, I., Reaction of Graphite with Sulfuric Acid in the Presence of KMnO4. *Russ. J. Gen. Chem.* **2005**, *75*, 162-168.
(5) Toyo Tanso Carbon-Graphite Products: Perma-Foil Graphite Sheet. www.tanso.se/wp-content/uploads/2017/08/Graphite-foil.pdf (accessed 28 October).
(6) Sara, R. V. Patent No. Ep0109839b1. Method of Making Graphite Electrodes. 1982.
(7) AM Carbon Graphite Anode Manufacturing Process. http://amcarbon.com/products/cathodic-protection/graphite/manufacturing-process/ (accessed 5 November).
(8) Alsmeyer, D. C.; McCreery, R. L., In Situ Raman Monitoring of Electrochemical Graphite Intercalation and Lattice Damage in Mild Aqueous Acids. *Anal. Chem.* **1992**, *64*, 1528-1533.
(9) Gordon, L., Us Company's Graphite Electrode Deals Signal Costs May Be Easing. *Metal Bulletin Daily* **2018**, 8-8.
(10) Alibaba.com Minerals & Metallurgy, Graphite Products, Graphite Sheets. https://www.alibaba.com/products/Graphite_foil/CID9090403.html?spm=a2700.7724838.12.2.75974dc5DOw00I&IndexArea=product_en (accessed 28 October).
(11) Industrial Minerals Staff Price Briefing: September 21-27. https://www.indmin.com/Article/3835204/Graphite/Price-Briefing-September-21-27.html (accessed 28 October).
(12) Novoselov, K. S.; Geim, A. K.; Morozov, S.; Jiang, D.; Zhang, Y.; Dubonos, S.; Grigorieva, I.; Firsov, A., Electric Field Effect in Atomically Thin Carbon Films. *Science* **2004**, *306*, 666-669.
(13) Novoselov, K.; Jiang, D.; Schedin, F.; Booth, T.; Khotkevich, V.; Morozov, S.; Geim, A., Two-Dimensional Atomic Crystals. *Proc. Natl. Acad. Sci. U. S. A.* **2005**, *102*, 10451-10453.
(14) Novoselov, K.; Geim, A. K.; Morozov, S.; Jiang, D.; Katsnelson, M.; Grigorieva, I.; Dubonos, S.; Firsov, A., Two-Dimensional Gas of Massless Dirac Fermions in Graphene. *Nature* **2005**, *438*, 197-200.
(15) Gurzęda, B.; Buchwald, T.; Nocuń, M.; Bąkowicz, A.; Krawczyk, P., Graphene Material Preparation through Thermal Treatment of Graphite Oxide Electrochemically Synthesized in Aqueous Sulfuric Acid. *RSC Advances* **2017**, *7*, 19904-19911.
(16) Gurzęda, B.; Florczak, P.; Kempiński, M.; Peplińska, B.; Krawczyk, P.; Jurga, S., Synthesis of Graphite Oxide by Electrochemical Oxidation in Aqueous Perchloric Acid. *Carbon* **2016**, *100*, 540-545.
(17) Parvez, K.; Rincón, R. A.; Weber, N.-E.; Cha, K. C.; Venkataraman, S., One-Step Electrochemical Synthesis of Nitrogen and Sulfur Co-Doped, High-Quality Graphene Oxide. *Chem. Commun.* **2016**, *52*, 5714-5717.
(18) Markovic, Z. M.; Budimir, M. D.; Kepic, D. P.; Holclajtner-Antunovic, I. D.; Marinovic-Cincovic, M. T.; Dramicanin, M. D.; Spasojevic, V. D.; Perusko, D. B.; Spitalsky, Z.; Micusik, M.; Pavlovic, V. B.; Todorovic-Markovic, B. M., Semi-Transparent, Conductive Thin Films of Electrochemical Exfoliated Graphene. *RSC Advances* **2016**, *6*, 39275-39283.
(19) Yu, P.; Lowe, S. E.; Simon, G. P.; Zhong, Y. L., Electrochemical Exfoliation of Graphite and Production of Functional Graphene. *Curr. Opin. Colloid Interface Sci.* **2015**, *20*, 329-338.
(20) Rao, K. S.; Sentilnathan, J.; Cho, H.-W.; Wu, J.-J.; Yoshimura, M., Soft Processing of Graphene Nanosheets by Glycine-Bisulfate Ionic-Complex-Assisted Electrochemical Exfoliation of Graphite for Reduction Catalysis. *Adv. Funct. Mater.* **2015**, *25*, 298-305.
(21) Abdelkader, A. M.; Kinloch, I. A.; Dryfe, R. A. W., High-Yield Electro-Oxidative Preparation of Graphene Oxide. *Chem. Commun.* **2014**, *50*, 8402-8404.
(22) Liu, J.; Yang, H.; Zhen, S. G.; Poh, C. K.; Chaurasia, A.; Luo, J.; Wu, X.; Yeow, E. K. L.; Sahoo, N. G.; Lin, J.; Shen, Z., A Green Approach to the Synthesis of High-Quality Graphene Oxide Flakes via Electrochemical Exfoliation of Pencil Core. *RSC Advances* **2013**, *3*, 11745-11750.
(23) Singh, V. V.; Gupta, G.; Batra, A.; Nigam, A. K.; Boopathi, M.; Gutch, P. K.; Tripathi, B. K.; Srivastava, A.; Samuel, M.; Agarwal, G. S.; Singh, B.; Vijayaraghavan, R., Greener Electrochemical Synthesis of High Quality Graphene Nanosheets Directly from Pencil and Its SPR Sensing Application. *Adv. Funct. Mater.* **2012**, *22*, 2352-2362.
(24) López-Díaz, D.; López Holgado, M.; García-Fierro, J. L.; Velázquez, M. M., Evolution of the Raman Spectrum with the Chemical Composition of Graphene Oxide. *The Journal of Physical Chemistry C* **2017**, *121*, 20489-20497.
(25) Nakajima, T.; Matsuo, Y., Formation Process and Structure of Graphite Oxide. *Carbon* **1994**, *32*, 469-475.
(26) Beck, F.; Jiang, J.; Krohn, H., Potential Oscillations During Galvanostatic Overoxidation of Graphite in Aqueous Sulphuric Acids. *J. Electroanal. Chem.* **1995**, *389*, 161-165.
(27) Bottomley, M.; Parry, G.; Ubbelohde, A.; Young, D., 1083. Electrochemical Preparation of Salts from Well-Oriented Graphite. *Journal of the Chemical Society* **1963**, 5674-5680.

(28) Lu, J.; Yang, J.-x.; Wang, J.; Lim, A.; Wang, S.; Loh, K. P., One-Pot Synthesis of Fluorescent Carbon Nanoribbons, Nanoparticles, and Graphene by the Exfoliation of Graphite in Ionic Liquids. *ACS Nano* **2009**, *3*, 2367-2375.
(29) Parvez, K.; Wu, Z. S.; Li, R.; Liu, X.; Graf, R.; Feng, X.; Müllen, K., Exfoliation of Graphite into Graphene in Aqueous Solutions of Inorganic Salts. *J. Am. Chem. Soc.* **2014**, *136*, 6083-6091.
(30) Yang, S.; Brüller, S.; Wu, Z.-S.; Liu, Z.; Parvez, K.; Dong, R.; Richard, F.; Samorì, P.; Feng, X.; Müllen, K., Organic Radical-Assisted Electrochemical Exfoliation for the Scalable Production of High-Quality Graphene. *J. Am. Chem. Soc.* **2015**, *137*, 13927-13932.